NOVA SCHOOL OF SCIENCE & TECHNOLOGY

DEPARTAMENT OF PHYSICS

DANIEL FILIPE MARIM DOS SANTOS

Bachelor Degree in Sciences of Physics Engineering

Development of Cryostats with Temperature Control for Electrical Characterization of Thin Films in the Range 77-300 K

MASTER'S IN PHYSICS ENGINEERING

NOVA University Lisbon

SEPTEMBER 2022

NOVA SCHOOL OF SCIENCE & TECHNOLOGY

DEPARTAMENT OF PHYSICS

Development of Cryostats with Temperature Control for Electrical Characterization of Thin Films in the Range 77-300 K

DANIEL FILIPE MARIM DOS SANTOS

Master/BSc in Physics Engineering

Adviser: Paulo Ribeiro
Associate Professor, FCT-NOVA University Lisbon

Co-advisers: Grégoire Bonfait,
Full Professor, FCT-NOVA University Lisbon

Examination Committee:

Chair: Dr. André Wemans
Assistant professor, FCT-NOVA

Rapporteurs: Dr. Maria Andrade
Associate Professor, FCT-NOVA University Lisbon

Adviser: Dr. Paulo Ribeiro,
Associate Professor, FCT-NOVA University Lisbon

MASTER'S IN PHYSICS ENGINEERING

NOVA University Lisbon
September 2022

Development of Cryostats with Temperature Control for Electrical Characterization of Thin Films in the Range 77-300 K

This document was created with Microsoft Word text processor and the NOVA thesis Word template.[1]

[1] https://github.com/joaomlourenco/novathesis_word/raw/master/novathesis_word-FINAL-EN.pdf.

ACKNOWLEDGMENTS

I want to express my gratitude to my supervisors, Professor Grégoire Bonfait and Professor Paulo Ribeiro, for all the support and guidance while developing this challenging thesis. I would also like to thank Professor Maria Raposo and Professor Susana Sério, who helped a lot throughout this period.

I wish to thank Mr. Afonso and Mr. Fábio for their help making all the electric circuits and cables and Mr. Faustino for building the pieces necessary to develop this thesis.

A big thanks to my colleagues who survived the MIEF with me, particularly my close friends Leonor, Rita, Inês, Teresa, Diogo and Nuno, for the times passed stressed studying for the next test and for the fun times playing cards and nights out.

A special thanks to my family, especially my mother, father and brother, who help and supported me during these long five years of study.

"What we know is a drop, what we don’t know is an ocean"

(Isaac Newton)

ABSTRACT

In this thesis, cryogenic systems capable of measuring thin film electric characteristics at low temperatures (77-300 K) were developed. Building in total three different prototypes capable of precise temperature control using liquid nitrogen as a cold source. Two prototypes measure the AC impedance of the samples and a third one measures the sheet resistance.

These systems are capable of obtaining the impedance value of DNA and graphene oxide thin films and the indium and fluorine doped tin oxides (ITO, FTO) sheet resistance. The study of such samples is essential to future sensor development, opening ways to improve the efficiency of these sensors.

In this thesis, we monitor the DNA and graphene oxide thin film impedance values increase with temperature decrease. Analyzing the DNA results, it was possible to build an equivalent electric circuit for this thin film, observing the Warburg component of the film. Regarding the ITO and FTO sheet resistance measurements a decrease with temperature was observed.

Keywords: Impedance spectroscopy, Temperature control,
Low temperature Electric characteristics

RESUMO

Nesta tese foram desenvolvidos de sistemas criogénicos capazes de fazer uma caracterização elétrica de filmes finos a baixas temperaturas (77-300 K). No total três protótipos diferente foram construídos, capazes de um controlo preciso da temperatura usando azoto líquido como fonte fria. Dois destes protótipos conseguem obter a impedância da amostra e um terceiro capaz de obter a resistência folha da amostra.

Após a construção destes sistemas, estes foram utilizados para medir a impedância de filmes finos de DNA e óxido de grafeno e a resistência-folha de substratos de óxidos de estanho dopados com índio e flúor (ITO, FTO). O estudo destes diferentes tipos de amostras é importante para desenvolvimento futuro de sensores, permitindo melhorar a eficácia destes.

Nesta tese, observa-se o aumento dos valores de impedância, dos filmes finos de DNA e óxido de grafeno, com a diminuição da temperatura. Observando os resultados obtidos do DNA foi possível fazer a representação de um circuito equivalente, no qual existe uma componente de Warburg no filme de DNA. Quanto às medições de resistência-folha do ITO e do FTO, observa-se uma diminuição destes valores com a temperatura.

Palavras chave: Espectroscopia de impedância, Controlo de temperatura,
Caracterização elétrica a baixa temperatura

CONTENTS

LIST OF FIGURES

List of Tables

ACRONYMS AND INITIALISMS

DC	Direct Current
AC	Alternate Current
DNA	Deoxyribonucleic Acid
GO	Graphene Oxide
IDEs	InterDigitated gold Electrodes
RT	Room Temperature
LT	Low Temperature
LN2	Liquid Nitrogen
USB	Universal Serial Bus
GSP	Gold plate Spring Probes
PEI/GO	polyethylenimine of Graphene Oxide
ITO	Indium-doped Tin Oxide
FTO	Fluorine-doped Tin Oxide

SYMBOLS

$\boldsymbol{R}$	Resistance
$\boldsymbol{\Delta V}$	Voltage Difference
$\boldsymbol{I}$	Current
$\boldsymbol{Z(\omega)}$	Impedance in function of frequency
$\boldsymbol{\theta}$	Phase difference
Z_R	Resistor impedance
Z_C	Capacitor impedance
Z_L	Inductor impedance
$\boldsymbol{R_S}$	Sheet resistance
$\boldsymbol{\rho}$	Resistivity

1

INTRODUCTION

Electrical characterization of materials is essential for their physical understanding and future technology development. Various characteristics can be measured and studied in different samples. Such as:

- Volume Resistivity (Ω/cm)
- Surface Resistivity ($\Omega/\square$)
- Dissipation Factor ($\%$)
- Break Down Voltage (kV)

These electrical characteristics present a temperature variation. This work aims to build a system that enables precise temperature control, allowing to study the variation of some electrical properties of different samples with the temperature, namely in the 77-300 K range.

1.1 Framework and Motivation

In the past, systems that allowed measuring impedance at low temperatures were already developed in the physics department, namely in the Laboratory of cryogenics (LIBPhys) [1, 2]. However, those systems did not have temperature control.

Systems that allow temperature control within an extensive range are already commercially available. For example, the system "129610A $\mathrm{LHe/LN_2}$ Cryostat" developed by Solartron. This system works in 77-600 K, using liquid nitrogen, with a precision of 0.05 K [3, 4]. However, this system is an expensive piece of machinery, developing a custom-made cryostat becomes much cheaper and will create the possibility to improve it through time and specifically to the exact searches needed in the future.

1.2 Contribution to Future Goals

The development of this system will allow a controlled study of different samples, such as graphene sheets, metallic oxides, and organic molecules. Such a study is essential for posterior sensor development, allowing us to understand various sensors optimal work point and working limits, improving future technology.

2

IMPEDANCE SPECTROSCOPY - SOME CONCEPTS

2.1 Resistance/Impedance

Ohm's law defines the resistance in terms of the voltage and direct current ratio (DC).

$$R = \frac{\Delta V}{I} \tag{2.1}$$

However, some materials are not only resistive when submitted to an alternate current (AC). Those materials present a capacitive and inductive component, presenting a more complex behavior denominated as impedance.

The impedance is the system's AC response to an AC signal imposed on the system [5]. As in DC systems, the impedance is expressed as the ratio between voltage variation and current variation. Impedance can be considered the AC analog to DC resistance, with the critical difference between the two being that the impedance includes a phase difference between the current and voltage, θ [6].

$$Z(\omega) = \frac{V(t)}{I(t)} = \frac{V_0 \sin(\omega t + \theta)}{I_0 \sin(\omega t)} \tag{2.2}$$

2.1.1 Complex algebra

The impedance can be represented using complex cartesian coordinates:

$$Z = Z_{re} + iZ_{im} \tag{2.3}$$

where $Z_{re}$and Z_{im} are the real and imaginary parts of $Z(\omega)$, respectively.

The impedance can also be represented in polar form:

$$Z = |Z|e^{i\theta} \qquad Z = |Z|(\cos(\theta) + isen(\theta)) \tag{2.4}$$

where $|Z|$ is the magnitude of Z and θ is the phase angle. The magnitude of Z and θ, can be calculated in the following manner.

$$|Z| = \sqrt{(Z_{re})^2 + (Z_{im})^2} \tag{2.5}$$

$$\theta = \arctan^{-1}\left(\frac{Z_{im}}{Z_{re}}\right) \tag{2.6}$$

A representation of the components can be seen in the Figure 2.1.

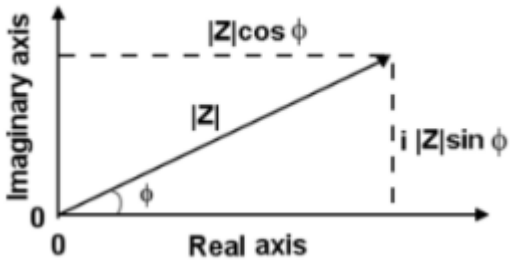

Figure 2.1: Representation of Z in the complex plane [5].

For pure resistive circuits (R), there is always a direct proportionality between the tension and current, respecting Ohm's law, not presenting a correlation with the frequency. Hence the impedance of the resistor circuit only offers a real component:

$$Z_{re} = Z_R = R \tag{2.7}$$

Considering an only capacitive circuit (C), the AC current in the capacitator is proportional to the rate of change of $V(t)$ and capacitance of the capacitor, which is:

$$I(t) = C\left(\frac{dV(t)}{dt}\right) = \omega C V_{max}\cos(\omega t) \tag{2.8}$$

Since $\sin(x) = \cos(x - 90°)$, we can rewrite the equation showing that $I(t)$ is $-90°$ out of phase with $V(t)$, and using the polar form for a more straightforward calculation, we can conclude:

$$Z_C = \frac{V_{max}\, e^{i\,0°}}{I_{max}\, e^{i\,90°}} = \frac{V_{max}\, e^{i\,0°}}{\omega C V_{max}\, e^{i\,90°}} = \frac{e^{i\,(-90°)}}{\omega\, C} \tag{2.9}$$

$$Z_C = -\frac{i}{\omega C} \tag{2.10}$$

The impedance of a pure capacitor has only an imaginary component that is inversely proportional to the product of ω and capacitance.

In an only inductive circuit, the inductor generates voltage $V(t)$ when a current $I(t)$ passes through it. Using the Faraday's law, the voltage is proportional to the rate of change current passing through the inductor of value L.

$$V(t) = L\left(\frac{dI(t)}{dt}\right) = \omega L I_{max}\cos(\omega t) \tag{2.11}$$

Like the capacitor circuit, the cosine indicates that the current and voltage are out of phase, but in inductor system the $I(t)$ is displaced $+90°$ with V(t).

$$Z_L = \frac{V_{max}\, e^{i\,90°}}{I_{max}\, e^{i\,0°}} = \frac{\omega L I_{max}\, e^{i\,90°}}{I_{max}\, e^{i\,0°}} = \omega L\, e^{i\,90°} \tag{2.12}$$

$$Z_L = i\omega L \tag{2.13}$$

The impedance of a pure inductor circuit has only an imaginary component, as the capacitor, which is proportional to ωL.

Resuming the impedance of purely resistive, capitative and inductive, circuits are respectively:

$$Z_R = R \qquad Z_C = -\frac{i}{\omega C} \qquad Z_L = i\omega L \tag{2.14}$$

Where impedance provided by capacitance and inductance are imaginary component and the pure resistive are real components, using equations 2.14 in 2.5 and 2.6, we obtain:

$$|Z| = \sqrt{(Z_R)^2 + (Z_L + Z_C)^2} \qquad \theta = \arctan^{-1}\left(\frac{Z_L + Z_C}{Z_R}\right) \tag{2.15}$$

$$|Z| = \sqrt{(R)^2 + \left(i\omega L - \frac{i}{\omega C}\right)^2} \qquad \theta = \arctan^{-1}\left(\frac{i\omega L + \frac{i}{\omega C}}{R}\right) \tag{2.16}$$

2.2 Impedance Spectroscopy

The impedance spectroscopy analysis studies the material's resistive, capacitive, and inductive impedance components. To analyze these components, a sinusoidal voltage is applied, generating a phase difference. This phase difference is expressed as radians or degrees and is necessary to measure the impedance.

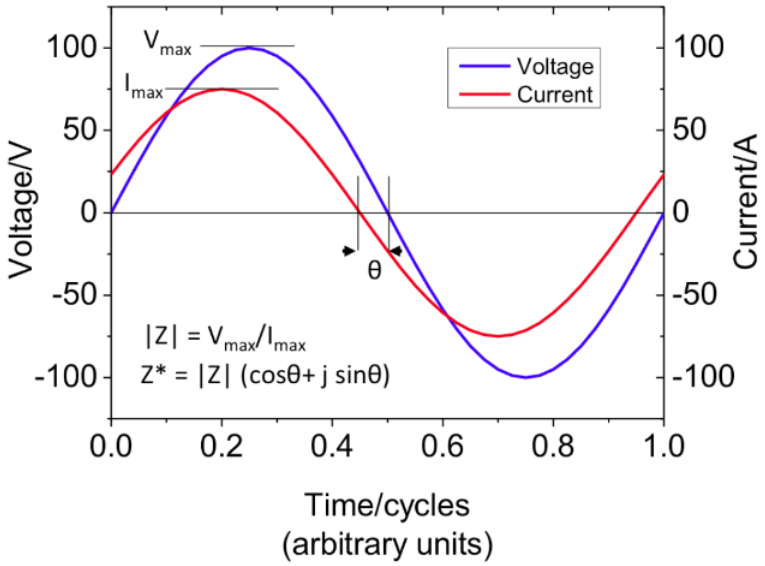

Figure 2.2 Relationship between the phase and magnitude of current and voltage sinusoids [6].

The impedance data is usually presented in the Nyquist and Bode plots. During this thesis, we will show the results using mainly Bode diagrams, representing $\log(Z)$ as a function of $\log(\omega)$, describing the frequency dependency on the modulus. And the Nyquist plots to display the real and imaginary parts of the impedance for n point measured.

In Figure 2.3 some typical behaviors that can occur in the imaginary/real Nyquist plots can be seen. Some of these forms will be explained in the next section (2.2.1.1), and also appear in thin film samples measured, analyzed in this thesis.

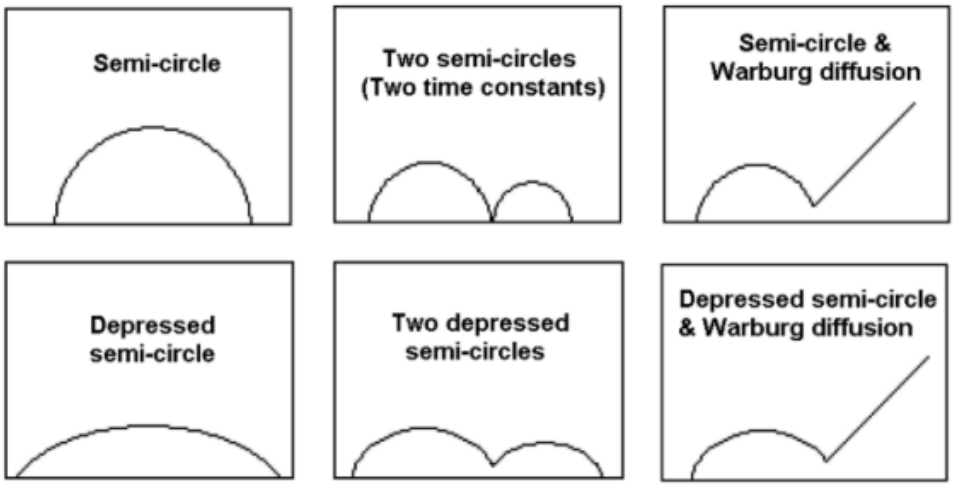

Figure 2.3: Nyquist plots of Imaginary and real components [5].
Semi-circles are obtained for RC circuits

2.2.1 Bode Plot/ Equivalent Circuits

Impedance analysis is done by fitting the sample data to an equivalent electric circuit model. An equivalent circuit model combines resistors, capacitors, and inductors, in series or parallel. In electrochemical and organic samples Warburg diffusion elements can also be involved.

Analyzing the simplest circuits, as present in Figure 2.4, is fundamental to understand the information of the equivalent circuit model. During this thesis, a circuit equivalence to an inductor component did not appear in the samples studied. That is why it is not represented on the following circuits, although it has a logic similar to conductor circuit model.

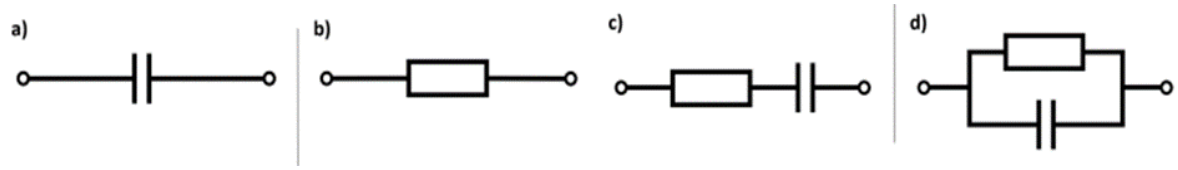

Figure 2.4: Representation of simplest circuits.

a) Capacitor, b) Resistor, c) Capacitor and Resistor in Series, d) Capacitor and Resistor in Parallel [2]

The impedance value of a capacitor (Figure 2.5 a)) is inversely correlated with the frequency, this is because when the capacitor is fully charged, it tends to oppose the current flux, as shown by capacitors equation (2.14). On the other hand, the impedance of a resistor (Figure 2.5 b)) is independent of the frequency, because current flux opposition strength is an intrinsic characteristic of resistors, as shown by resistor equation (2.14).

In circuits with more than one component, the impedance value depends on how the circuit is assembled, mainly where the current tends flow. In series circuits (Figure 2.4 c)), the impedance value is controlled by the component with the higher resistance in a specific frequency (Figure 2.5 c)). Furthermore, the impedance value in parallel circuits (Figure 2.4 d)) is controlled by the branch with the lowest current resistance in due frequency (Figure 2.5 d)).

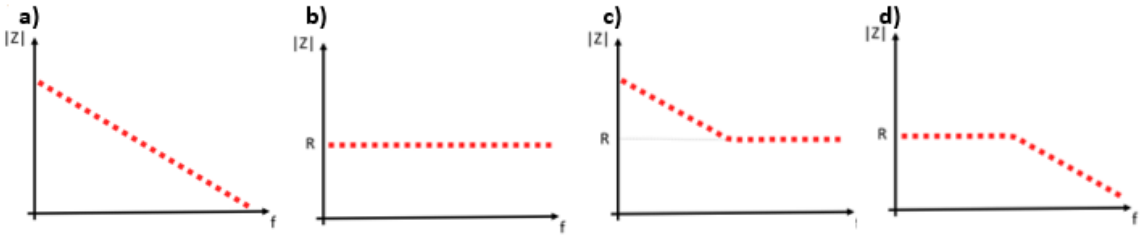

Figure 2.5: Bode plot of the impedance modulus as a function of frequency in simplest circuits.

a)Capacitor, b) Resistor, c) Capacitor and Resistor in Series, d) Capacitor and Resistor in Parallel [2].

2.2.1.1 Impedance of Semi-circle and Warburg Element

The impedance data of a sample is often described by an equivalent circuit relevant to the conditions of the experiment, using circuit elements that represent various physical processes [7]. During the development of this work, two meaningful equivalent circuits need to be considered, the ones represented in Figure 2.6 a) and Figure 2.7 a).

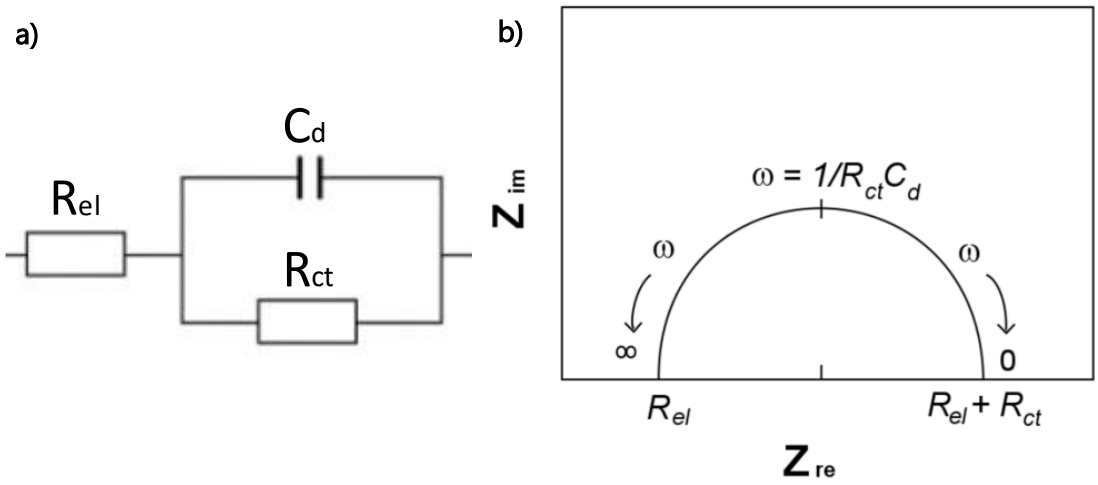

Figure 2.6: Semi-circle impedance.
a) Circuit resistor and capacitor in parallel, b) correspondent Nyquist plot [5].

The impedance associated with the circuit in Figure 2.6 a), leads to a semicircular Nyquist curve Figure 2.6 b). When the frequency tends to infinity, the impedance of the capacitor branch tends to zero in equation (2.14), meaning that the only component influencing the current route is R_{el}. Conversely, when the frequency tends to zero, the capacitor branch impedance tends to infinity, forcing the current through the remaining branch, resulting in an impedance value of $R_{el}+R_{ct}$, which means the higher the value of R_{ct} the higher the radius of the semi-circumference. In both these frequency extremes, the impedance originated from the capacitor is zero, therefore not presenting imaginary values and intercepting the real axis in the Nyquist plot. The Nyquist curve's highest imaginary value occurs when both branches equally divide the current corresponding to the characteristic frequency of the circuit. On the left side of the maximum imaginary value, the current mainly passes by the capacitor branch, and on the right side of the maximum imaginary value, the current passes mainly by the resistor branch.

The circuit represented in Figure 2.7 differs from the previous one because it has a Warburg diffusion element in the resistor branch. It is important to highlight that the Warburg impedance cannot be described (in an equivalent circuit representation) by any combination of capacitors and resistors [7], or other usual electronic components.

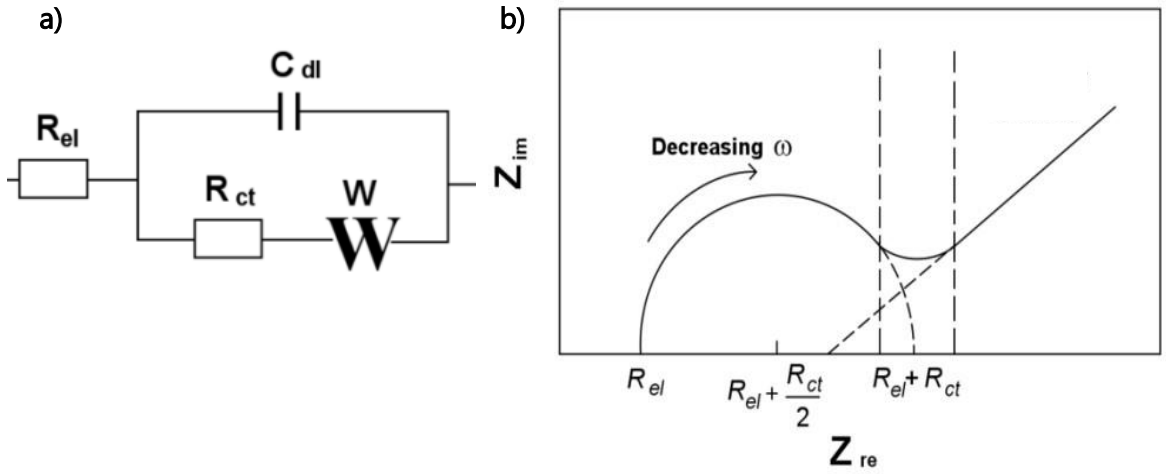

Figure 2.7: Warburg element impedance
a) Circuit equivalence to DNA thin film, b) correspondent Nyquist plot [5].

The Warburg diffusion element represents the diffusion that occurs at low frequency when performing measurements with an impedance spectrometer. At low frequency, the low potential values are held long enough, reducing the number of conducting species (electrons, ions) in front of the electrode. This reduction is relevant because due to the lack of species close to the electrode, it is harder to the current to flow, using the same potential, increasing the impedance measured. The Warburg impedance is visible in the Nyquist plot as a straight line with a 45° angle with the real axis (Figure 2.7 b)).

In this thesis, when analyzing a DNA film in section 4.3.2, an equivalent circuit model is built, using a software called ZView. Since the Warburg impedance cannot be represented as a combination of resistors and capacitors, ZView defines the Warburg impedance element with three components, W_P, W_T, and W_R. W_P is a fixed value of 0.5 that defines the Warburg element as being finite length Warburg. W_T is a value characteristic of the study sample being calculated as $W_T=L^2/D$ (in which L is the effective diffusion thickness, and D is the effective diffusion coefficient of the particle). W_R is a parameter that defines when the Warburg impedance starts to appear in the Nyquist plots, being proportional to the value of $R_{ct.}$

2.3 4-Point Method

The 4-Point Probe Method, also known as Kelvin sensing, allows one to measure the sheet resistance and consecutively calculate the resistivity of thin layers, provided there are satisfied some primary sample conditions such as the homogeneity of the sample and constant thickness [8].

This method consists of four independent electrical probes placed along a straight line and separated by a constant distance (s). The two external probes apply a current to the sample, while the two internal probes measure the potential drop between them. Due to not passing current in the internal probes, the resistance intrinsic to the wires and the contacts of the probes with the sample is not counted in the measurement. Considering an ideal infinite thin film of thickness t, the resistivity (ρ) and the sheet resistivity (R_s) are calculated with the following formula [9]:

$$R_s = \frac{\rho}{t} = \frac{\pi}{\ln(2)}\frac{V}{I} = 4.532\left(\frac{V}{I}\right) \tag{2.17}$$

The thin film can be considered infinite if its length and width are forty times longer than the distance between the probes (s). Since we don't follow these required dimensions when calculating and the sheet resistance, it is necessary to multiply the previous equation by a geometric correction factor, this geometric correction factor depends on the dimension of the sample (L, W) and the distance between probes (s).

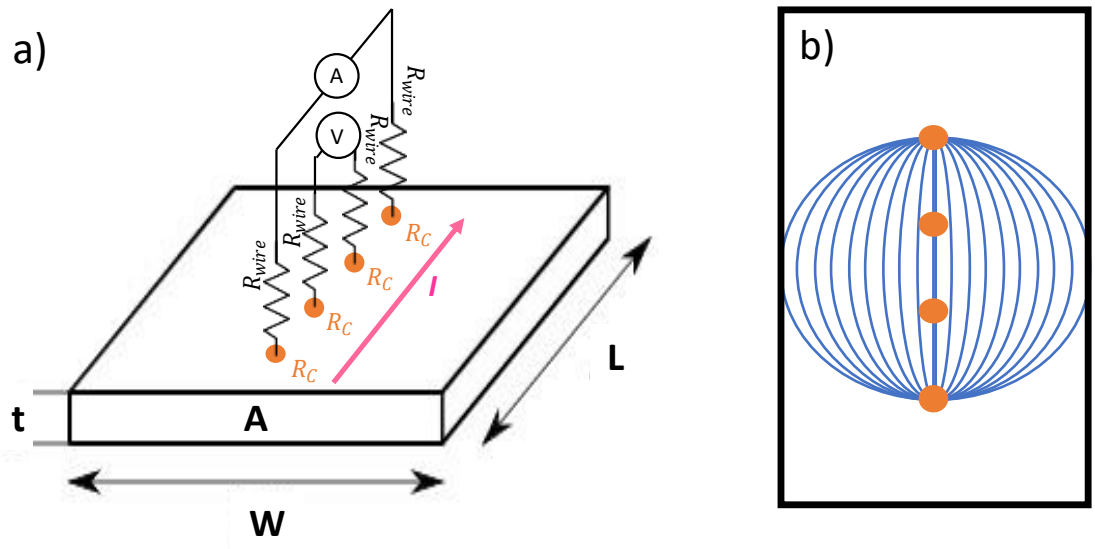

Figure 2.8: Electrical circuit diagram of the 4-Point method.
a) Representation of 4-point method, with R_C as contact resistance and R_{wire} as wire resistance. b) Sketched the current/electric filled lines in such a configuration.

2.3.1 Sheet Resistance

Sheet resistance is measured using the 4-Point Method, and it is a very useful measurement because it enables us to compare the electrical properties of samples with different dimensions.

While the resistance is a three-dimension measurement, the sheet resistance is not dependent of the sample size and represents the sheet resistance of a square (L=W), distinguish of the intrinsic resistivity by its units Ω/□ (read as "Ohm per square").

The resistance and the sheet resistance have the following relation:

$$R = \rho \frac{l}{A} = \rho \frac{l}{Wt} = \frac{\rho}{t} \frac{l}{W} = R_s \frac{l}{W} \tag{2.18}$$

where R is the resistance, L is the length, A is the cross section that can be split in W with and t thickness, as shown in Figure 2.8. So, is possible to obtain the resistivity and resistance values, using the sheet resistance, if the sample dimensions are known.

3

MATERIALS AND METHODS

3.1 Interdigitated Sensors

To measure the electrical properties of DNA and graphene oxide (GO), thin films interdigitated gold electrodes (IDE) over ceramic substrate were used. These interdigitated gold electrodes are composed of two gold electrodes that can be represented as one capacitor of value 100 pF. These IDEs offer several advantages, such as working with samples of low volume and avoiding tedious polishing of solid electrodes. Furthermore, the chain configuration, where the thin film is deposited, enhances sensitivity and detection limits [10].

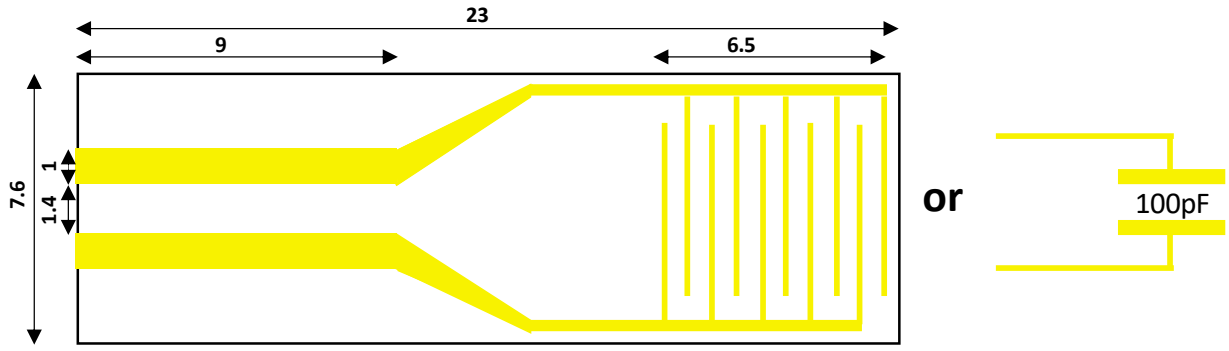

Figure 3.1: Interdigitated gold electrode. Representation of interdigitated sensor on the left, with chain visible on the right side of the IDE, with dimension in mm. And equivalent electric circuit on the right

3.1.1 DNA Film

The DNA thin film, as shown in Figure 3.2, was prepared using 10 mg of DNA extracted from lyophilized calf thymus DNA (cas number 73049-39-5). For the purpose of making a

DNA sensor, 500 µL of ultrapure water was used to dissolve the DNA. Then, the DNA solution was gently mixed and left to rest in the fridge for 30 min. After that, using a micropipette, 50 µL were deposited in the interdigitated area of the sensor. Finally, the sensor was left in a dark and closed environment with silica for 2 h, to remove the water from the solution by evaporation.

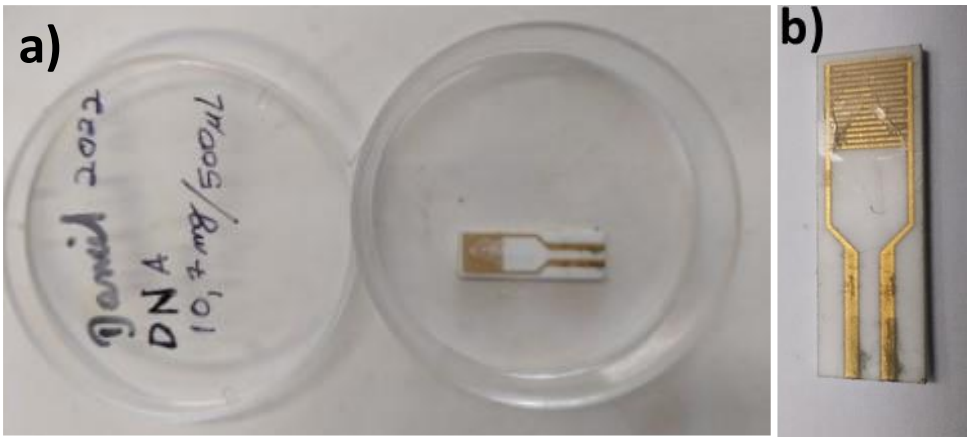

Figure 3.2: Interdigitated electrode with thin DNA film. Different perspectives of DNA thin film a) and b)

3.1.2 Graphene Oxide Film

The graphene oxide (GO) thin film, as shown in Figure 3.3, was prepared by removing 450 µl graphene oxide from the ALDRICH case, with a concentration of 4 mg/mL in water. Then the 450 µl were directly deposited in the interdigitated sensor, not diluting the solution more than it was any further. Finally, the solution was left to dry in a dark and closed environment with silica during the night, for about 10 h, with the same purpose that when making a DNA film, to evaporate the water from the sensor.

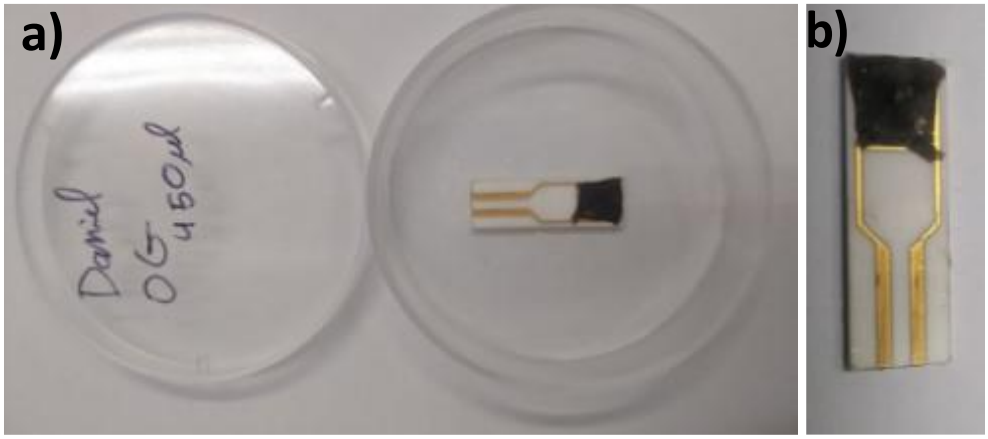

Figure 3.3: Interdigitated electrode with thin GO film. Different perspectives of GO thin film a) and b)

3.2 Impedance Spectrometer

The impedance spectrometer used during the development of this project was the *1260A impedance analyzer* coupled to a *1296A Dielectric interface* system from AMETEK Scientific instruments, as seen in the Figure 3.4. These two instruments were controlled by a computer using the interface software SMaRT. A scheme of how it is assembled is shown Figure 3.8.

The *1260A impedance analyzer* is an apparatus that measures the output spectrum of systems relative to an input signal. It measures the magnitude and phase relationship between the input and output signal, testing the sample over a wide frequency range of 10 μHZ to 32 MHz [11]. However, the equipment 1260A is not capable of measuring impedance for materials with low conductivity, especially at low frequencies.

So, the *1296A Dielectric Interface* overcomes these limitations allowing for accurate measurements for all kinds of highly resistive materials such as: polymers, ceramics, ion conductors, dielectrics, piezo/ferroelectrics, among others, also allowing to preform measurements in the frequency range to 100 MΩ (10^8 Ω) - 100 TΩ (10^{14} Ω) [12].

Figure 3.4: Impedance spectrometer instruments.
1296A dielectric interface on the 1260A impedance analyzer

3.3 Temperature Monitoring

3.3.1 Pt100

Pt100 resistors are platinum sensors that have an excellent correlation between temperature and (DC) electrical resistance. Denominated as such because, at 273.15 K or 0°C, they have a resistance value of 100 Ω. The precise sensor correlation, temperature versus resistance in 70 K to 300 K temperature range and their low price are the reason why these sensors were chosen to monitor the temperature in our cryogenic systems.

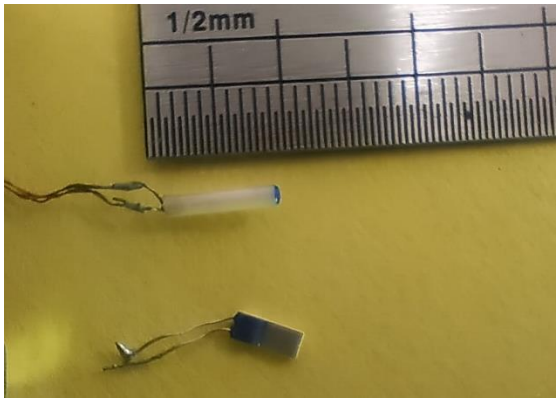

Figure 3.5 Pt100 resistors

For measuring the resistance in the sensor Pt100, the 4-point method is used. As explained before, this method is more suitable because it eliminates the wire resistance from the measurement, measuring only the potential difference between the sensor terminals, turning more precise the temperature measurement.

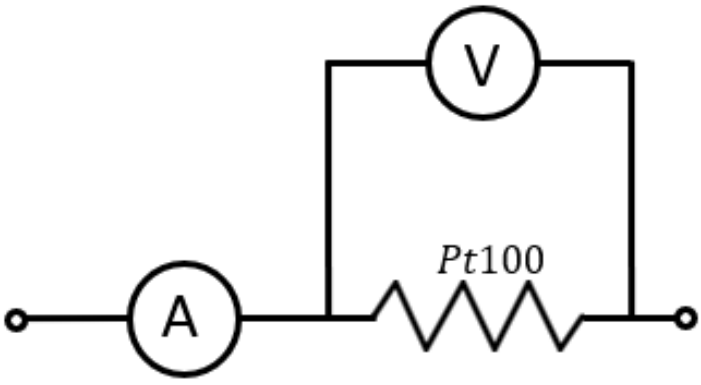

Figure 3.6: Schematization of 4-Point method used in the platinun sensors

3.3.2 Temperature Controller LakeShore 332

The Model 332, depicted in Figure 3.7, is a temperature controller manufactured by the Lakeshore company. This device offers the possibility to easily measure the temperature with a high resolution of 1 K for two separated sensors. It also has two independent control circuits, one with a 50 W (50 V/ 1 A) and the other with a 10 W (10 V / 1 A) output, that allow working according to the value measured by the input chosen sensor [13].

This Model also has a significant advantage because it allows a line of communication with the SMaRT software used to measure the impedance, allowing a more straightforward way to measure electrical impedance with temperature. Although this direct communication is possible, a more flexible approach was chosen to analyze the data, being the temperature data followed in the device LakeShore 332 and the impedance analyzer data in the software SMaRT. A scheme of how the devices are connecter is shown in the Figure 3.8.

Figure 3.7: Temperature controller Model 332

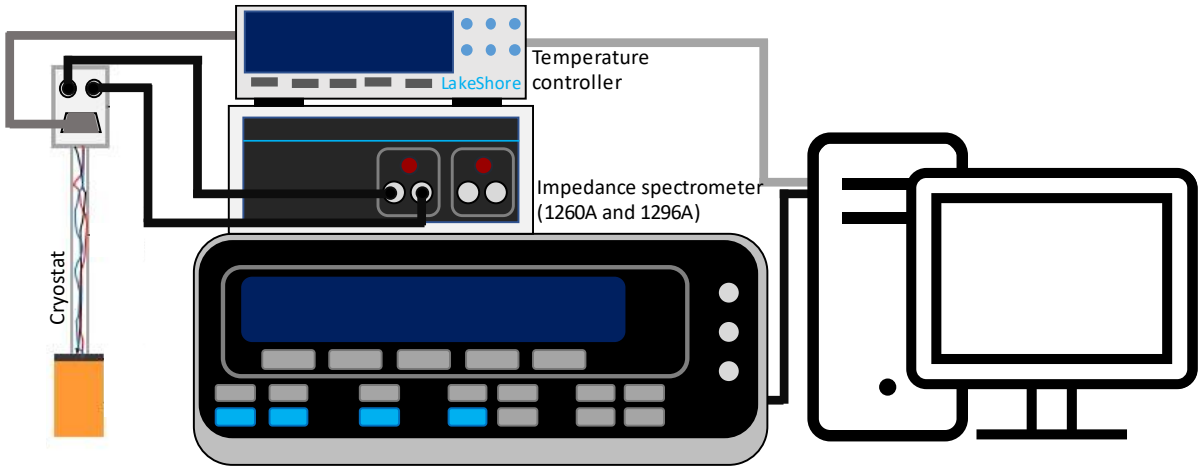

Figure 3.8: Scheme between the different devices required for impedance measurement with the cryostat

3.3.3 LabVIEW Interface

As means to interact with the temperature controller Lakeshore 332, a LabView interface was developed. Beyond the indication of the two sensors temperature values, this interface displays three graphs showing the temperatures, the temperature slope, and the output power used for temperature control in percentage, all in function of time (only one is shown in the figures). It includes, also a main panel seen in Figure 3.9, where the main commands can be seen and control, such as: the setpoint, the output power range (High, medium, or low), the maximum slope value considered for temperature stability check, the liquid nitrogen level in the dewar. In this panel a more automatic way to make different successive temperature steps (stair control), can also be applied. To simplify the communication and mobility of Model 332, the LabView program was developed to communicate via GPIB or RS232.

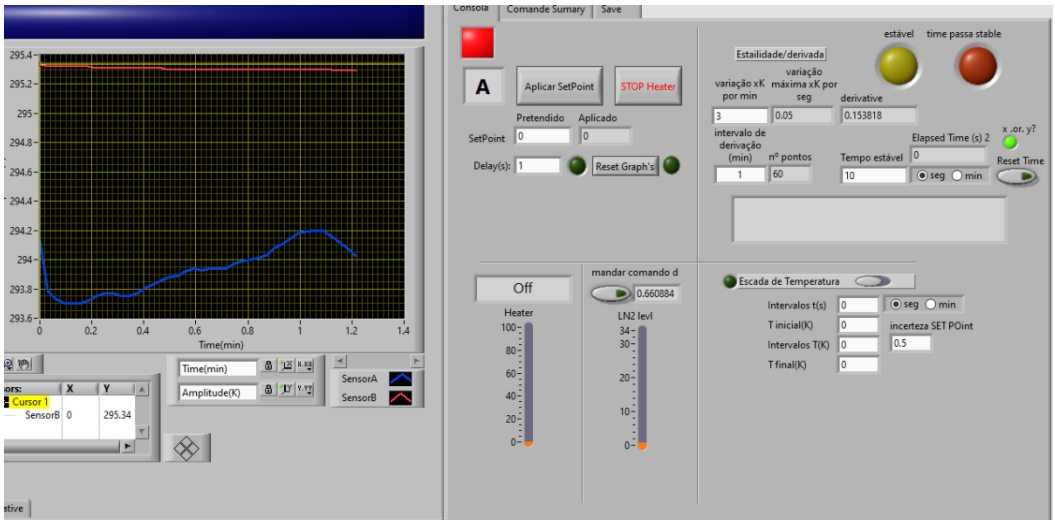

Figure 3.9: Main panel control temperature

This interface has two more secondary panels, the command summary and the save panels.

The command summary in Figure 3.10 contains the main panel's information, and the controls typically kept the same for the all experiment, defined at the beginning. Such as the sensor used for temperature control, the units of temperature to use, the output power scale (low, medium, or high), and if the setpoint changes gradually or instantly (ramp mode), among others.

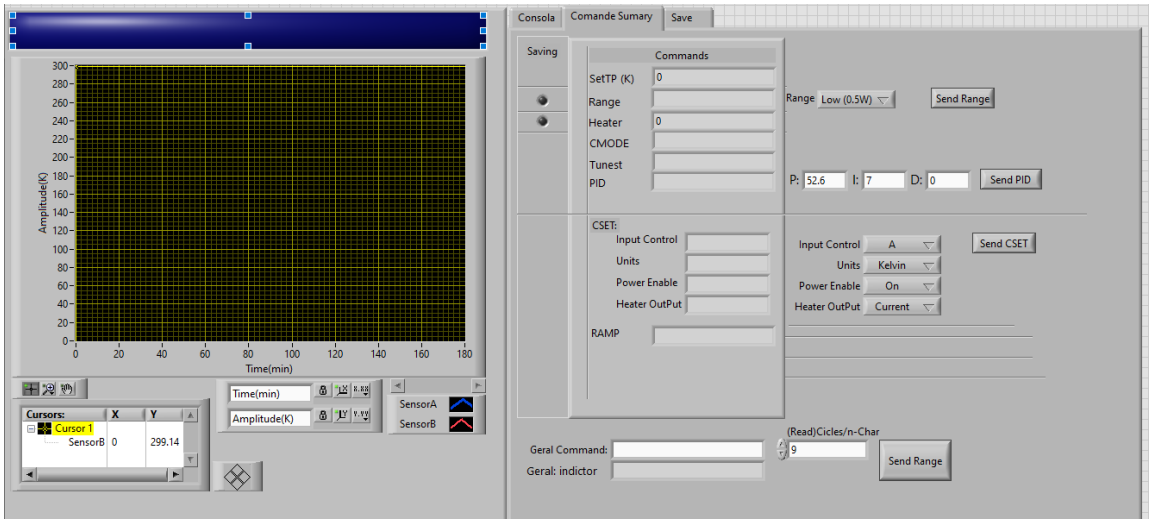

Figure 3.10: Control summary panel control temperature

Finally, the third panel is responsible for the data saving process in Figure 3.11, confirming if it is saving, where it is being saved, and what variables measured want to be saved. Also, it defines if it saves all variables from the data measured through time or only when the temperature is stable, being also possible to keep both types of data.

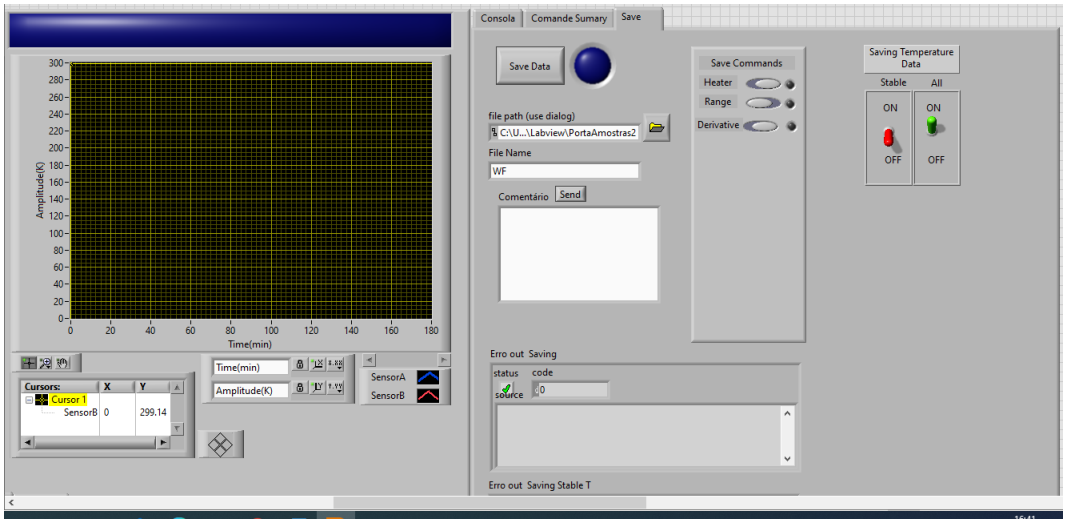

Figure 3.11: Save panel control temperature

3.4 Cryogenic System Construction

As said before, this project is based on systems developed in the Laboratory of Cryogenics of the Physics Department [1, 2]. In both projects, the systems were capable of electrical characterization (DC [1] and AC [2]) and have a similar constitution, as seen in Figure 3.12.

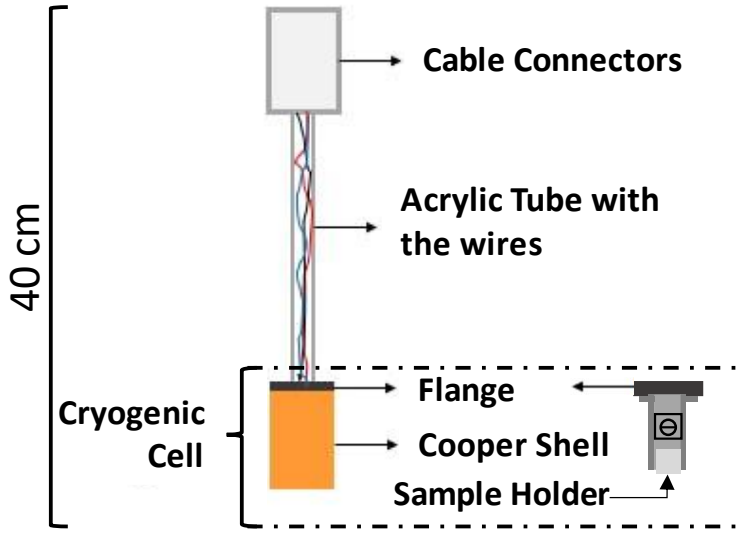

Figure 3.12: Base schematic of the cryogenic system
with internal and external view of the cryogenic cell

These systems comprise three significant parts, the cryogenic cell, the tube in which the wires pass from room temperature (RT) to the cryogenic cell at low temperature (LT), and the cable connectors at RT. The cryogenic cell is composed of a copper shell, a flange, and a sample holder. In the cryogenic cell, the copper shell ensures a good heat flux transfer, temperature homogenization and protects the sample holder inside the copper shell from direct contact with liquid nitrogen. The flange is the support that sustains and fixes all the cryogenic cell components together. Finally, the cable connectors are fixed on a plastic or inox box and links the system to the electronic equipment at RT that will measure and analyze the data.

To perform measurements in the previous systems mentioned, shown in Figure 3.13, the cryogenic cell is initially cooled down by direct contact between the cooper shell and the liquid nitrogen (LN2) at 77 K, reaching this temperature. Eventually, the LN2 evaporates, and the cryogenic cell starts to warm slowly, reaching room temperature. These systems measurements are performed during the slow temperature increase, without temperature stabilization, shown in Figure 3.14.

These assemblies allow for a rapid sample replacement, being only necessary to unscrew the copper shell from the flange to access the sample holder.

The systems developed and described in this thesis will follow a similar structure but will allow to stabilize the temperature at any value. Prototype 2, described more ahead, escapes from this typical structure, still allowing temperature stabilization.

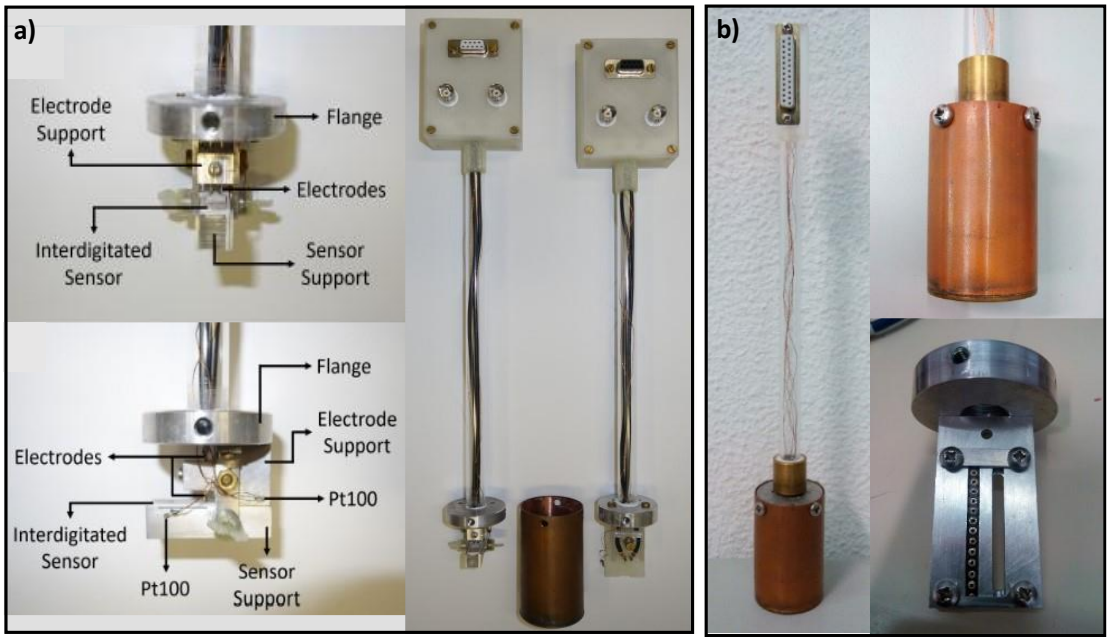

Figure 3.13: Systems and cryogenic cells of previous projects.

a) System capable of measure thin films in AC [2] and b)) System capable of measure wires in DC [1]

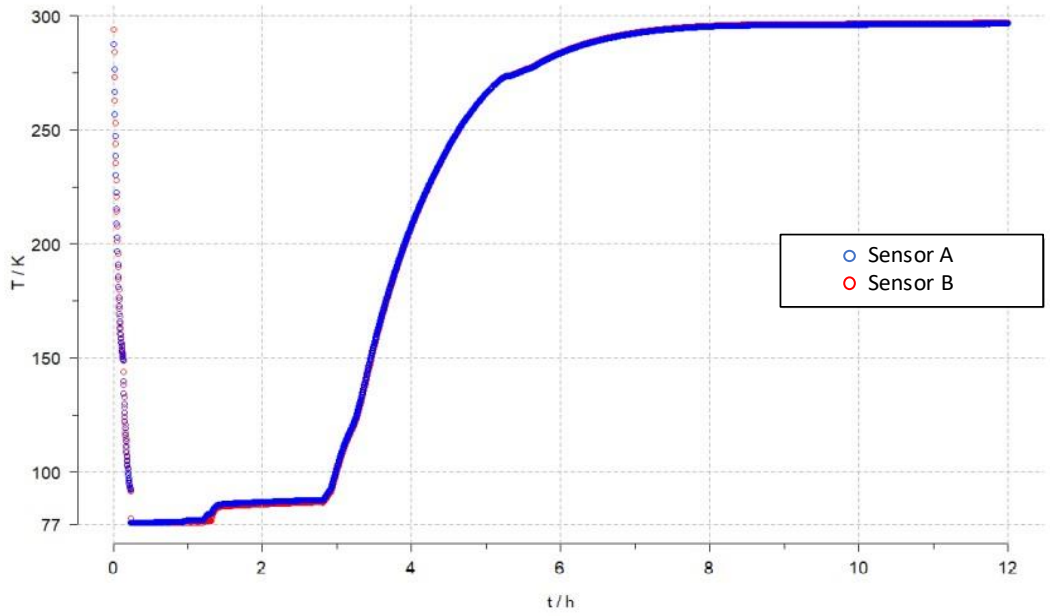

Figure 3.14: Temperature variation as function of time, used in the systems and cryogenic cells in Figure3.12

3.4.1 Thermal Insulation of the Cryogenic Cell

To control the system's temperature, it is necessary to establish a balance between a hot source and a cold source. In this project, the cold source will be the LN2. There are two design system possibilities, as seen in Figure 3.15.

The first possibility is to attach copper wires to the bottom of the copper shell, letting the cryogenic cell suspended above the LN2, allowing only the copper wires to be in touch with the LN2, these wires work as the cold source. And attach a set of heating resistors to the flange, working these ones has a hot source, as exemplified in Figure 3.15 a).

The second possibility, the one chosen and developed during this thesis, instead of using copper wires in contact with LN2 as a cold source, the entire cryogenic cell is used as a cold source, being the cryogenic cell involved in a thermal barrier and dipped in LN2. And like the first possibility, the heat resistors are attached to the flange or sample holder to work as a hot source, as exemplified in Figure 3.15 b).

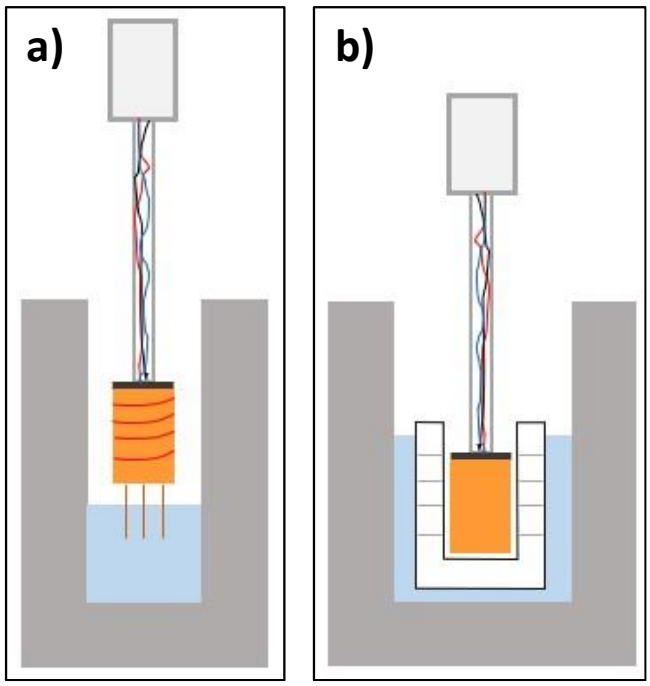

Figure 3.15: Prototypes structures possibilities schemes.
a) First possible structure, b) Second and developed structure.

This thermal barrier must provide a good thermal isolation avoiding liquid nitrogen from entering into direct contact with the copper all at the same time, preventing a noncontrolled rapid temperature decrease when dipped, and allowing to maintain the wanted temperature value, using a reasonable heating power. This barrier also allows the infiltration of some liquid nitrogen to allow it to cool the system without taking too much time and power to reach the required temperature. The balance of the heat resistor's power and the cold provided by the thermal barrier will allow a good temperature control and allowing different temperature steps to be created.

To achieve the ideal insulation barrier, multiple types of materials were tested. The protective barrier must protect the cryogenic cell from direct contact with LN2 but also allows

some nitrogen leaks to enter into contact with the copper through natural or artificial porosity channels.

For the first approach, a black sponge was used, letting the nitrogen flow by capillarity through the sponge's natural porosity. However, the flow was excessive, not allowing us to control the temperature of the sample holder above 110 K. By trying different materials and configurations, as seen in Figure 3.16, an adequate thermal isolation was achieved that allowed us to control the temperature of the cryogenic cell between 77 K and 300 K. The final isolation material chosen was polystyrene because it is a high isolative material, an easy material to work and less expensive, being used in house insolation. The copper shell was covered with a set of polystyrene donut shaped disks fixed to each other with aluminum tape.

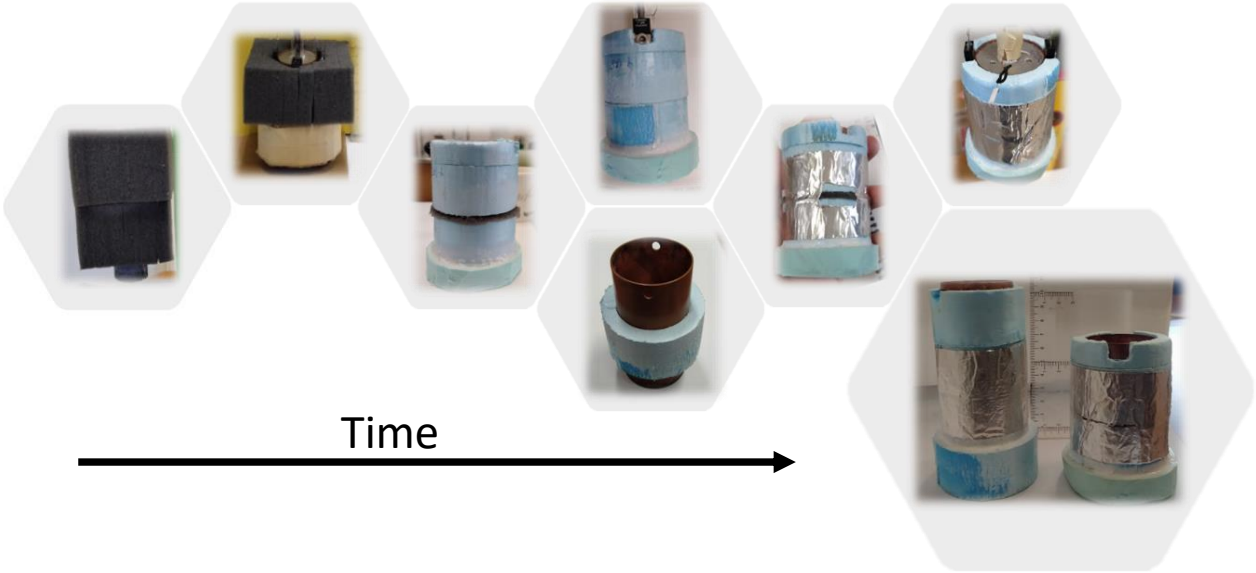

Figure 3.16: Thermal barrier evaluation, from left to right. Final version at the right

3.4.2 Prototype 1 Cryostat

For the construction of prototype 1, was used an assembly (sample holder) built in a previous thesis [2]. Prototype 1 is an aluminum structure with the IDE sample facing upward. Since the structure is made of aluminum, a 3D printed plastic cylinder isolates the contact cylindrical probes responsible for the electrical contact between the IDE and the copper wires, avoiding short circuits. The IDE sample is positioned between ledges with the appropriate interdigitated sample dimensions, forcing the correct alignment between the cylindrical probes and the samples. The probes used in this prototype and prototype 3 are gold plate spring probes (GSP), shown in Figure 3.17. The GSP is composed of two parts connect-

ed by a spring. When pressed, the spring of this probe ensures good electrical contact between the probe and the interdigitated sample, seen in Figure 3.18 a).

Figure 3.17: Golden spring probes.

An insulating barrier, shown in Figure 3.18 b) and described in section 3.4.1, was added to the assembly as well as a set of two 22 Ω heating resistors [14] in series, screwed on the aluminum flange. The insulation barrier is fixed around the copper shell while the heating resistors are on opposite sides of the flange, as seen Figure 3.18 a), transferring the heat from the flange to the sample holder.

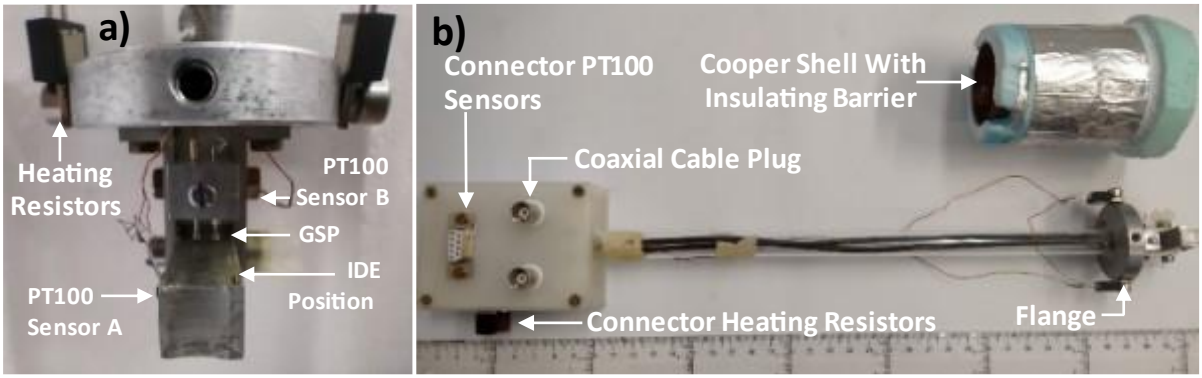

Figure 3.18: Pictures of Prototype 1.
a) Sample holder, b) Cryogenic Cell Exterior

Since the heat resistors are placed on the exterior of the cryogenic cell while performing the experimentation, it is necessary to be aware that the liquid nitrogen can not pass above the bottom of the flange. If that happens, the nitrogen enters in direct contact with the heat resistors, preventing to obtain the required temperature.

To monitor the liquid nitrogen level, a balance system was built using an arduino UNO microcontroller, and the force sensors of a low-cost commercial balance. This system converts the conjunct weight of the liquid nitrogen and the dewar to the nitrogen level, allowing the LabView to measure the LN2 level during the experiment.

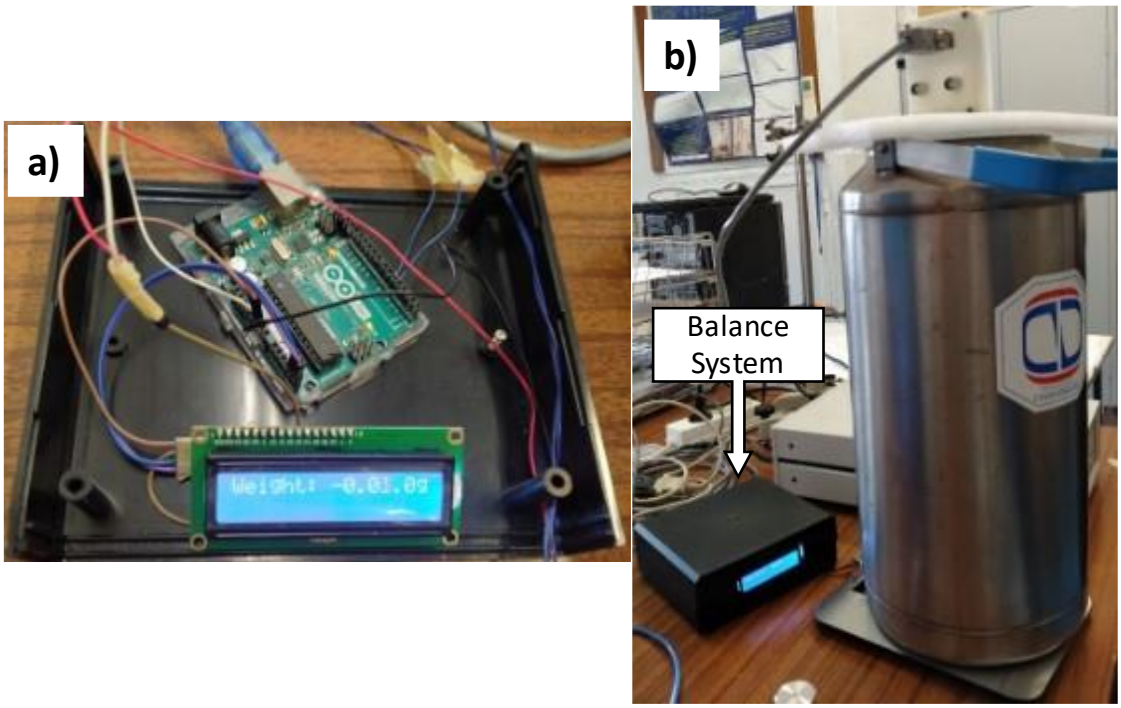

Figure 3.19: Balance system, used with prototype 1. a) System connections and b) System in operation

3.4.3 Prototype 2 Cryostat

The prototype 1 allowed a very good temperature control (see section 4.1.1) but presented two defaults. The first was the necessity of constant monitorization of the liquid nitrogen level, having a height range for optimal work, making it necessary to replenish liquid nitrogen, when out of the optimal range. Second, a strange and reproducible phenomenon occurs, in the experimental data, changing the impedance values after the colling process. Supposably due to water condensation, more about this phenomenon will be explained in section 4.3.2 of this thesis.

To try to correct these two principal short comings, another system was developed, with a significant number of changes to avoid the condensation of water in the sample holder and the need to monitor the LN2 level, also preventing direct contact between the nitrogen and the cryogenic cell. One of the changes made was using an adapted USB port to replace the probes used in prototype 1, shown in Figure 3.20 b) and c), allowing for an easier and more stable way to place and replace the samples. Moreover, this new probe type offers a larger electrical contact than the previous spring probes, generating less noise in the measured data.

Another change was to replace the principal cooling strategy by changing the system structure. The sample holder, unlike prototype 1, doesn't have a cooper shell and a polysty-

rene insulation barrier. The cryogenic cell is placed on the tip of an inox rod, in which the electrical wires pass through ending in a cable connector. Then the inox rod is placed inside a tube and closed. All the components mentioned are shown in Figure 3.20 a), making the hollow structure airtight. Then after these two pieces are assembled, and the entire system is placed inside the dewar liquid nitrogen. Since there is no direct contact between the sample holder and LN2, both liquid and gas, the sample is cooled by gaseous conduction through the existing gas in the tube (1 bar at 300 K to 700 mbar when the tube is in the LN2) and by thermal radiation. Since the sample is in an airtight place, when the system is cooled, the water condensation will be residual (limited to the H_2O quantity in the system before closing).

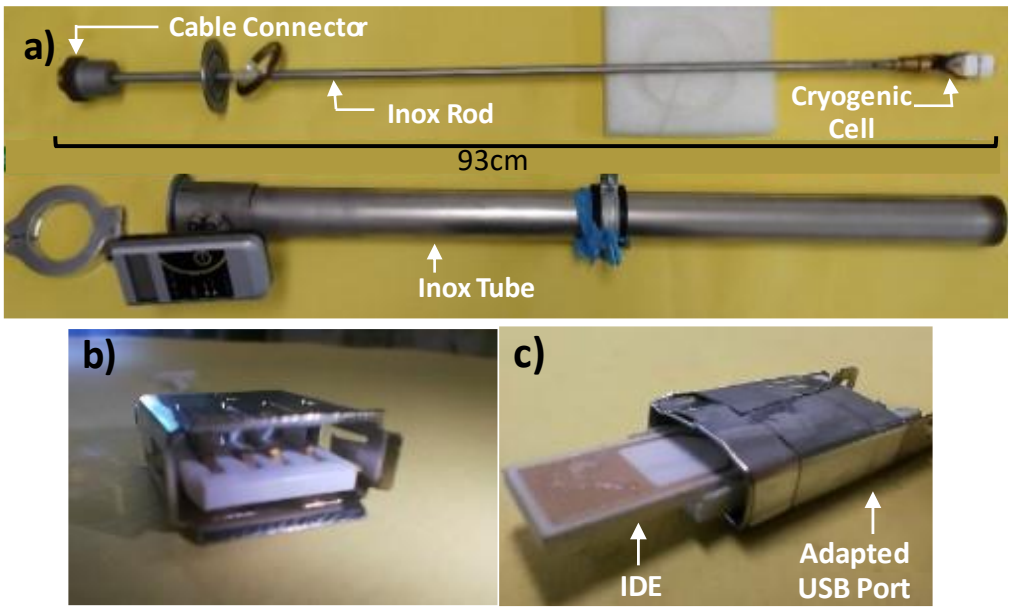

Figure 3.20: Major changes in the prototype 2.

a) Structure of prototype 2, on the top is the inox rod where the sample structure is put, on the bottom is the hollow structure that protects the sample from liquid nitrogen contact and is airtight when assemble. Adapted USB to replace previous probes b) Before modification, and c) After the modifications

The development of this prototype can be separated into two specific versions. The first version was the first try to build a sample holder capable of measurements using the USB probe. However, this version could not correctly measure, as demonstrated by the data in section 4.4.2, due to a lack of temperature uniformization through the cryogenic cell. The second version tries to resolve this problem.

3.4.3.1 Prototype 2, 1st Version

The first assembly of prototype 2 uses a brass support and two thermal resistances on opposite sides in the middle of the support. As prototype 1, two Pt100 sensors are used to monitor the temperature along the brass support and the IDE, positioned as represented in Figure 3.21. In this prototype, the sample holder is the adapted USB port, and when the IDE is placed on it, part of it stays suspended in the air, as seen in Figure 3.22 b) (annex A.1).

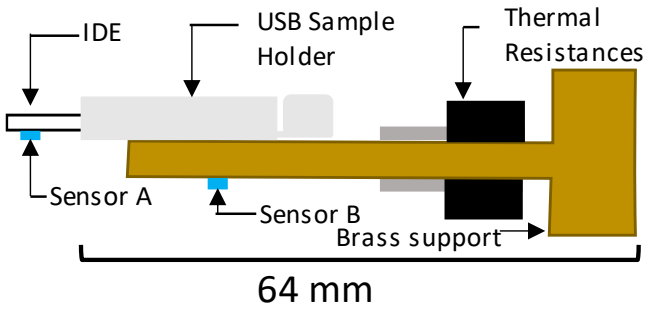

Figure 3.21: Lateral scheme of prototype 2 1st version cryogenic cell, and position of its different components

Before closing, the sample holder was wrapped in aluminum to ensure that the sample does not receive directly thermal radiation from the 77 K wall of the tube (Figure 3.22 c).

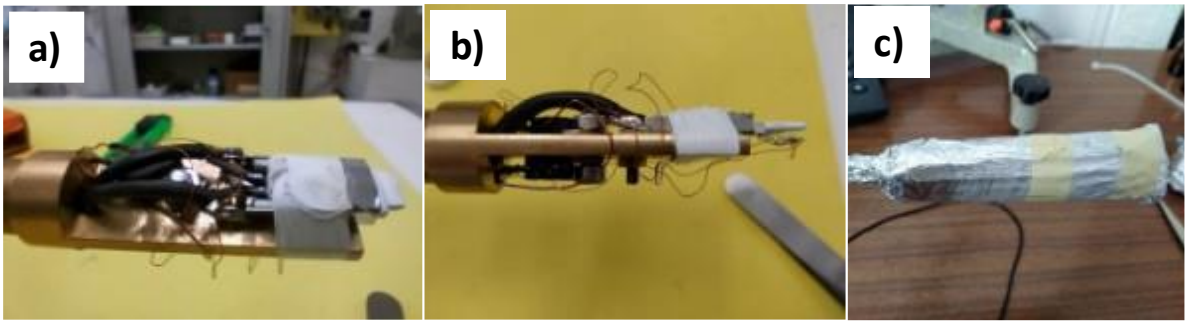

Figure 3.22: Assembled cryogenic cell in different perspectives.
a) Without Sample, b) With Sample, c) Wrapped by aluminum

3.4.3.2 Prototype 2, 2nd Version

After analyzing the data obtained using the first prototype, it was necessary to modify the cryogenic cell to permit a better temperature distribution along the brass support (more explanation in section 4.4), developing an improvised and simpler cryogenic cell. Using an aluminum plate, the brass support surface is extended and a new USB probe was built, reducing its size, as shown in Figure 3.23. The IDE is positioned in the aluminum, as showed in Figure 3.24 a) and b), not being suspended as in the first version making it easier for the heat flux to propagate throughout the film.

Although a final sample holder was not built, it was designed, present in annex A.2.

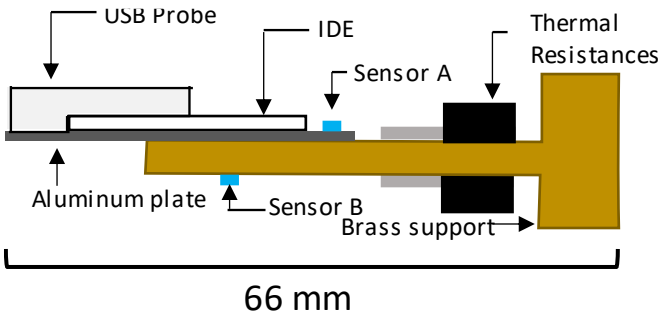

Figure 3.23: Lateral scheme of Prototype 2nd version cryogenic cell, and position of its different components

Figure 3.24: Cryogenic cell in different perspectives.

3.4.4 Prototype 3 Cryostat

Prototypes 1 and 2 were developed to measure the impedance using the impedance spectrometer Solartron, but other electric characteristics are interesting to measure, such as the sheet resistance, used to calculate the resistivity of the material in study. Using the same design as prototype 1, a new sample holder was developed that could support a different type of samples and the four probes necessary for measuring, depicted in Figure 3.25.

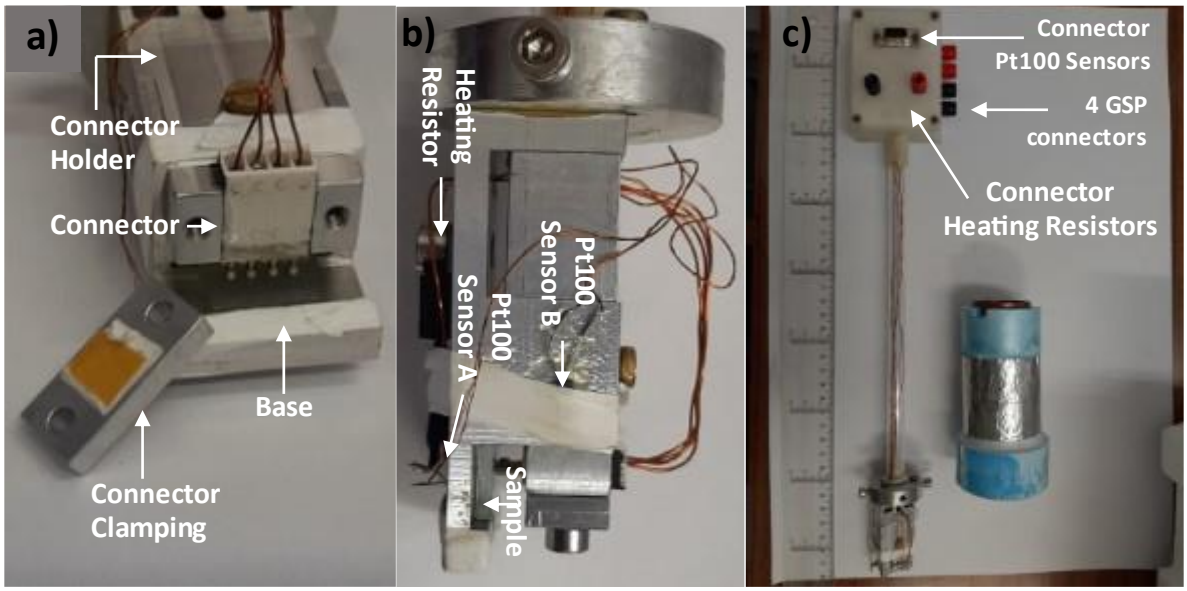

Figure 3.25: Pictures of Prototype 3.
a and b) Sample holder in different perspectives, c) Prototype 3 structure and cryogenic cell.

This sample holder is composed of three separated pieces, all of them made of aluminum seen in Figure 3.25 a). The first piece (annex B.1), is the base of the assembly, where the sample is positioned by sliding it on to a groove in the side of the base (Figure 3.25 b). This base is fixed to the flange by two screws, and a heating resistance is attached to the back of the base, as seen in Figure 3.25, being the piece where the heat flux will propagate. The second piece, the connector holder (annex B.2), is a movable piece located on the top of the base that moves perpendicular to the base. This piece has a spring system that ensures that the probes are well positioned and in contact with the sample (not seen in the Figures because it is inside the connector holder). Finally, the third piece, (annex B.3), is attached to the connector holder, clamping the white plastic piece, coming from a commercial connector, that holds firmly the four GSP probes.

3.5 Circuits and Connectors

To ensure the systems developed were measuring correctly, a reference circuit with a 100 kΩ resistor in series with a 10 nF capacitor, in parallel with a 100 pF capacitor, was made on a circuited printed board, as shown in Figure 3.26. By measuring this circuit with known variables, we can compare the data measured with the expected one.

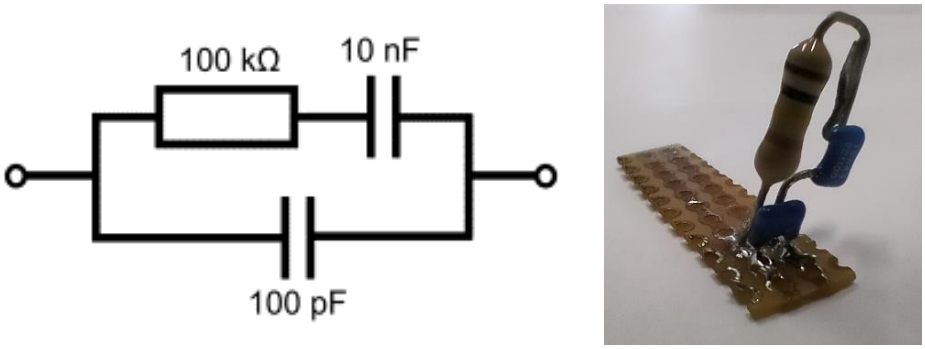

Figure 3.26: Reference circuit schematic and picture in printed board

Additionally, a circuit reference made by AMETEK SI (Figure 3.27 a)), with the same values, is also used to confirm the normal operation of the 1260A impedance analyzer.

Finally, additional tests were made using a blue connector normally used in the lab (Figure 3.27 b)).

It is essential to highlight that the comparison between our new systems with the reference ones (AMETEK and blue probe) can only be made at room temperature, since those do not support to be exposed to low temperatures.

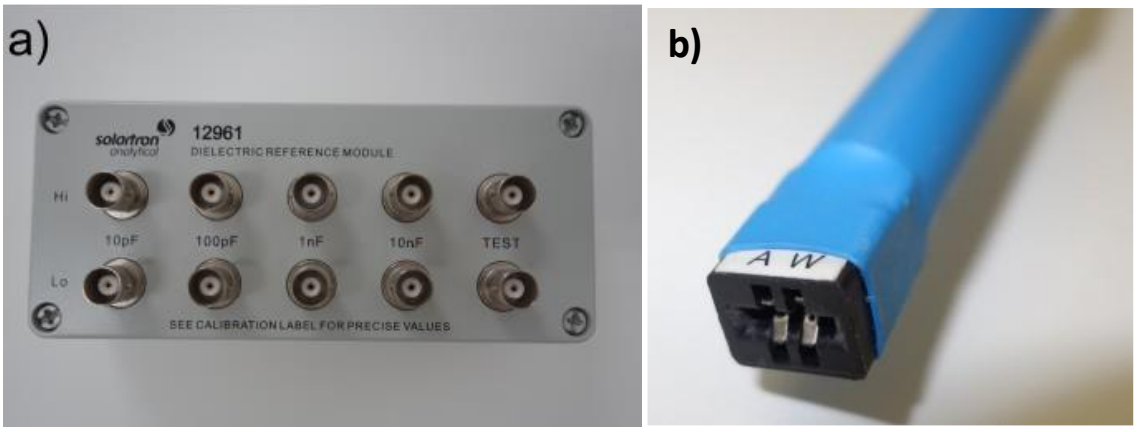

Figure 3.27: a) AMETEK reference circuit b) Blue probe

4

RESULTS AND DISCUSSION

In this section, we will describe the tests that validate that the cryogenic cell temperature control is working satisfactorily and if the measurement done using the sample holders designed and the different systems configurations are adequate for our measurements.

The experiments were performed using the impedance spectrometer 1260A and 1296A, through the SMaRT software, defining the parameters of 50 mV voltage amplitude and 0 V bias voltage, with thirty-one frequency points between 1 and 10^6 Hz.

The software SMaRT is used to obtain the measured impedance data, and the LabVIEW interface controls the temperature of the sample. A scheme how the devices are connecter is shown in the Figure 3.8.

4.1 Temperature Validation

During the development of this project, three prototypes were built in total. Prototypes 1 and 3 have essentially the same structure, prototype 1: Figure 3.18 a) and prototype 3: Figure 3.25 c), while prototype 2 is significatively different, Figure 3.20. Both these types of structures use the Lakeshore 332 to control the temperature of the sample holder, using the same LabVIEW program for both structures. But since the structure format impacts the temperature control, it was necessary to analyze the two control temperature structures separately.

4.1.1 Prototype 1 and 3

Prototypes 1 and 3 were made to study different electrical characteristics of thin films, however they have the same structure and use the same thermal barrier involving the cryogenic cell.

When performing the experiment, the dewar was filled up to 13 cm with nitrogen liquid (≈ 2.3 L, ≈ 1.9 kg), and then the system was introduced slowly inside the dewar, involving the cryogenic cell in liquid nitrogen. After inserting the cryogenic cell in nitrogen, the LabVIEW interface was used to control the temperature as seen in Figure 4.1, using two Pt100 type sensors A and B to monitor the temperature (Prototype 1: Figure 3.18, Prototype 3: Figure 3.25). First, the temperature drops slowly until it reaches 80 K, and from that point forward, the temperature is controlled in 20 K steps until it reaches 280 K.

The data obtained shows that reaching the minimum temperature of 80 K takes about 30 min, and it is possible to establish different temperature levels, taking no more than 10 min to stabilize each temperature level. Using steps of 20 K, it is possible to go from 80 K to ambient temperature in no more than 156 min, in other words, less than 2 h 36 min. Also, both sensors, Pt100 A and B, located in different places on the sample holder, present the same values, meaning that the heat is uniformly spread.

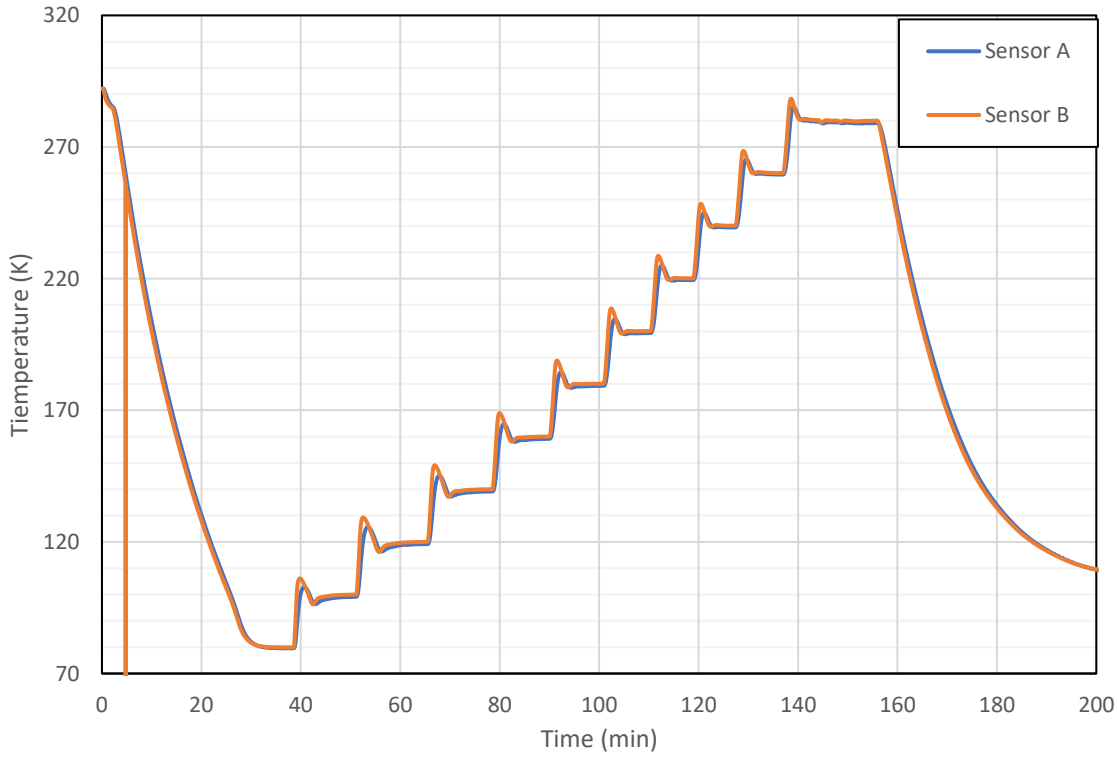

Figure 4.1: Graph Temperature stabilization for structure used in Prototype 1 and 3. Considered stabilized with a temperature variation lower then 3 K/min

It is also important to refer that it was not necessary to replenish the liquid nitrogen during this temperature variation, being possible to do two of these cycles of temperature variation without refilling.

4.1.2 Prototype 2

As described before, prototype 2 is the one that escapes the typical structure format used in the other structures developed. So, it was necessary to conduct a separate study to confirm if this structure is adequate for temperature control of the sample.

Such as the test of prototypes 1 and 3, liquid nitrogen was poured inside the dewar to the required level (not critical in this case), and then the assembled structure (Figure 3.20) was placed inside it. The temperature data obtained during this test is displayed in Figure 4.2, using, as the other two prototypes described above, two Pt100 sensors located in different parts of the cryogenic cell (Figure 3.21). As for the prototypes 1 and 3 test, first, the cryogenic cell reached the lowest temperature possible, then 20 K temperature steps were done until reaches room temperature (300 K).

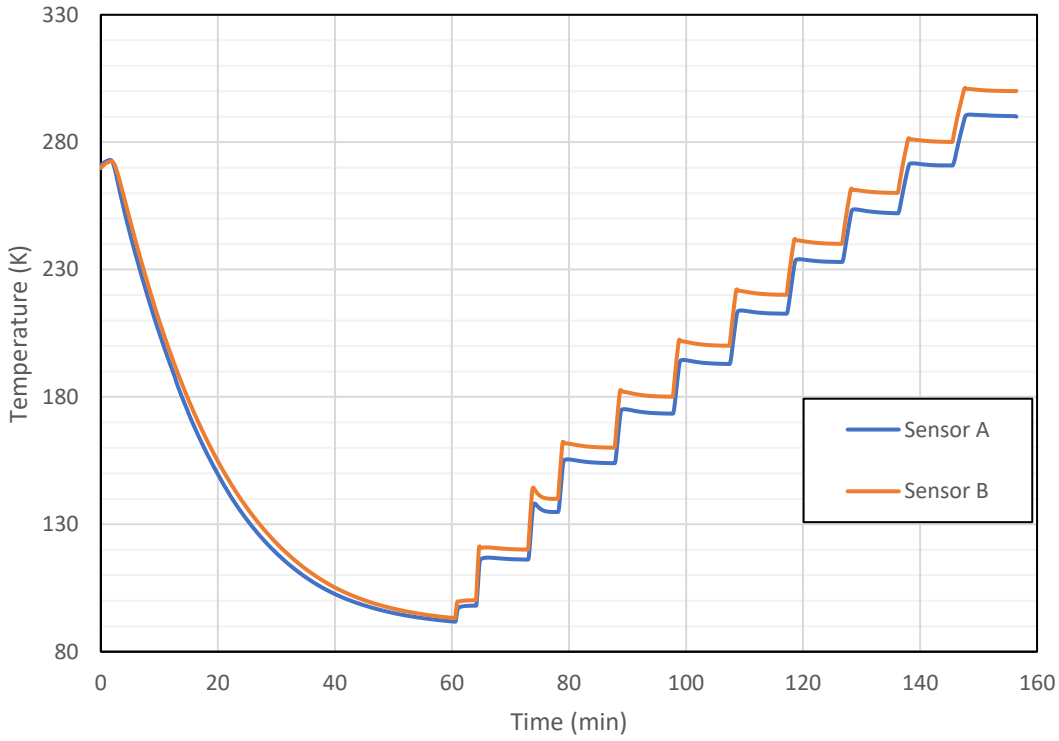

Figure 4.2: Graph Temperature stabilization for structure used in Prototype 2. Considered stabilized with a temperature variation lower then 3 K/min

The data obtained shows that the minimal temperature reached is 90 K and it was possible to achieve different temperature levels, taking no more than 5 min stabilize each set-points. Compared with the other structure of prototypes 1 and 3, this one has a higher minimum temperature but provides faster temperature control, reducing the measurement time

in a full range of temperatures. However, a significant temperature gradient exists along the temperature cell.

4.2 Circuit and Probes Validation

As said before, diverse types of cryogenic systems were used in this thesis. Before using those systems for sample characterization, it is necessary to confirm if they are working correctly. For that purpose, the circuits and connectors mentioned in section 3.5 are used.

The test circuit used to confirm the correct functioning is shown in Figure 3.26. The samples analyzed are thin films placed above an interdigitated electrode substrate. In this circuit, the 100 pF capacitor represents the substrate, while the branch with 100 kΩ resistance and 10 nF capacitor represent the components of the thin film. Testing the different probes and the different circuits, we get the data in Figure 4.3.

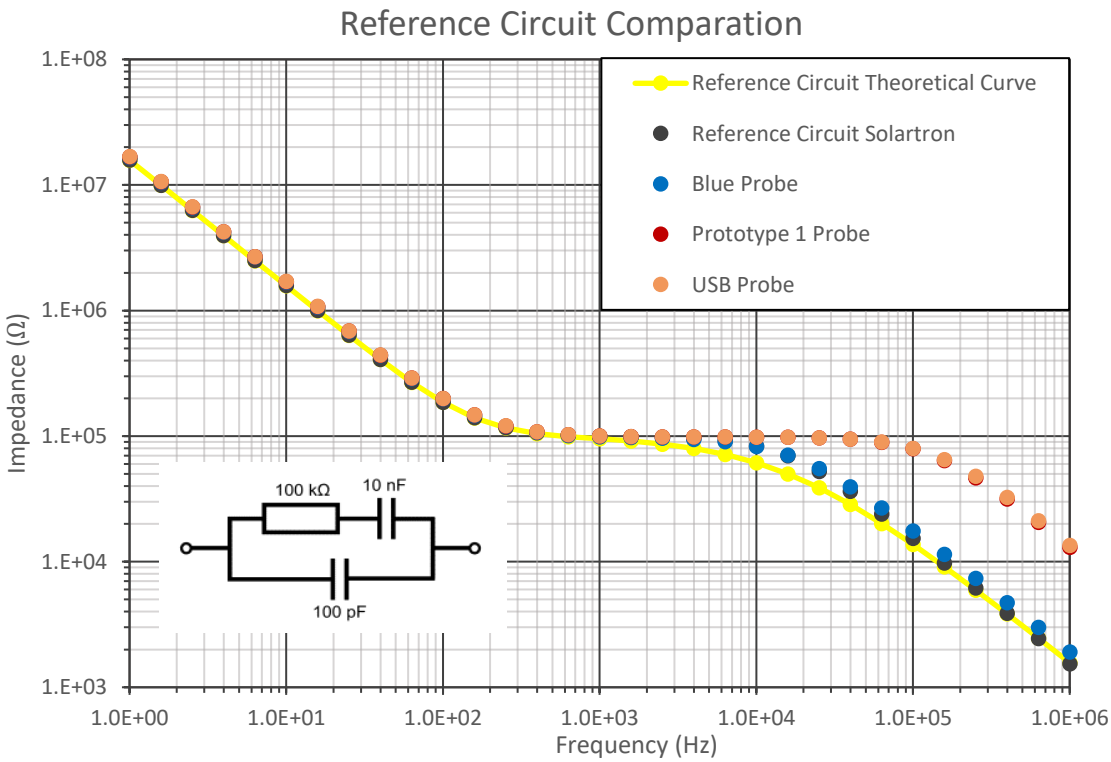

Figure 4.3: Bode plot of impedance of different probes with reference circuits

The curves obtained by the blue probe, the reference circuit Solartron, shown in Figure 3.27, and the theoretical curve have an excellent data overlap, concluding that the blue probe is working correctly. The curves obtained using prototype 1 probe and the USB probe presented a deviation of values at high frequency. This deviation means that there is some parasitical capacitance in series with the 100 pF element, reducing the original value of this

branch. Although it is an unexpected phenomenon, it does not present a serious issue because it only affects the capacitor that represents the substrate, not the values of the branch that represents the thin film we want to measure.

Also, an important aspect, before measuring impedance with the systems, is to know which is the most suitable AC voltage to apply to the system and if it changes with the temperature. The experiments that gave the results in Figure 4.4 were developed using a film of polyethylenimine of Graphene Oxide (PEI/GO) in prototype 1, varying the AC tension applied.

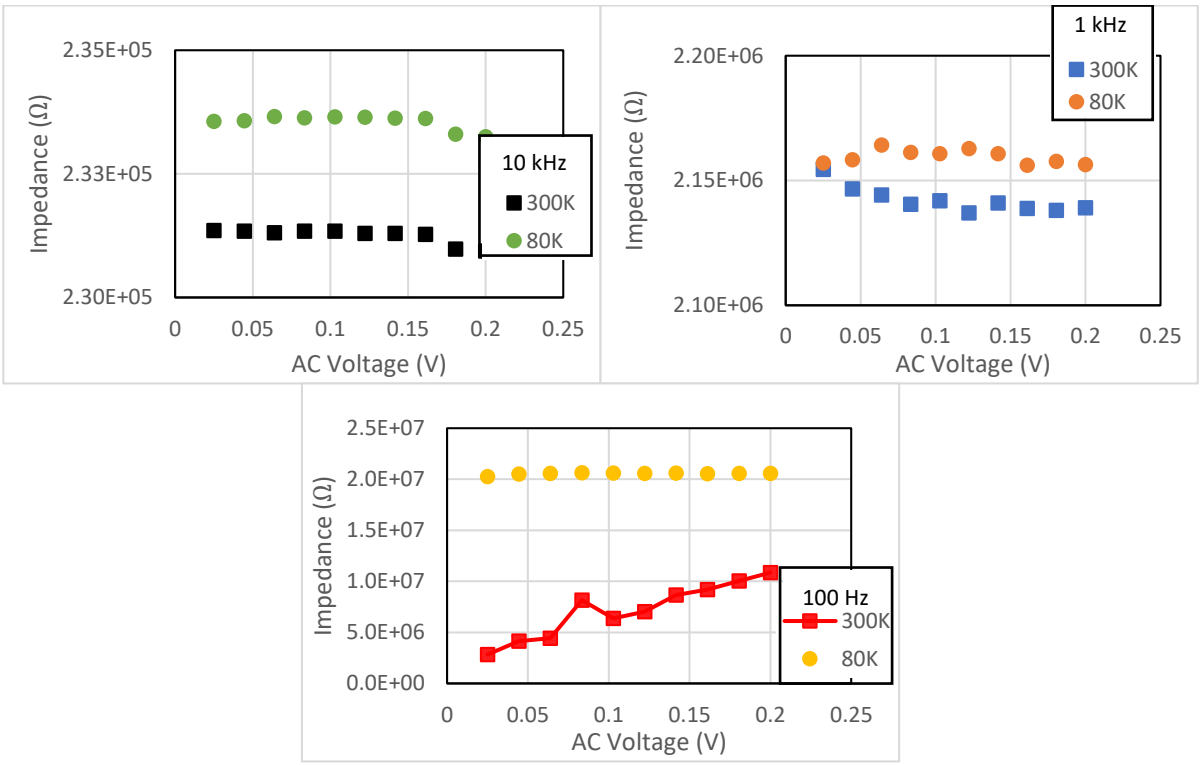

Figure 4.4: Electrical impedances as a function of AC tension, at fixed frequencies and for the two limit temperatures

With the results of the graphs in Figure 4.4, we can observe that the AC tension does not affect the value of the thin film impedance measured, except when carried out at 100 Hz and 300 K.

Since the results at 100 Hz and 300 K are the only results with impedance varying with the tension and it has a low frequency value, we conclude that these results were not correctly measured due to noise at low frequency, similar noise is also seen in Figure 4.5, and there is no immediate impact in the system measurements using different voltage values.

4.3 Prototype 1 Measurements

Prototype 1 was designed to study interdigitated electrode samples. Therefore, were studied a interdigitated substrate and thin films of DNA and graphene oxide, produced as mentioned in 3.1.

4.3.1 Substrate

The IDE is the substrate where the thin film is deposited, so it is essential to analyze it and its behavior at low temperatures. The IDE is expected not to show a variation of impedance with temperature. If it had, it would be necessary to consider that fact, when measuring the deposited films. Also, it is essential to compare the values obtained via the blue probe, using this one as a reference, obtaining the results in Figure 4.5.

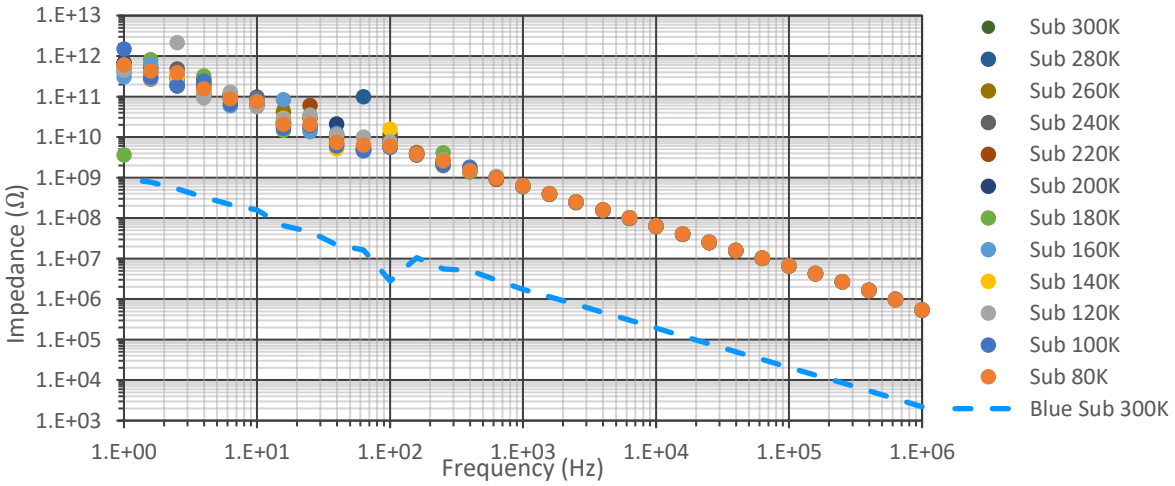

Figure 4.5: Bode plot of impedance at different temperatures for substrate using prototype 1

By analyzing this data, we can observe, as expected, that there is no significant change in the substrate data values when the temperature changes. There is a curve deviation between the data acquired by prototype 1 and with the blue reference probe. Considering the deviation that appeared in the data of Figure 4.3, this deviation was expected, but as explained before, this deviation only affects the substrate capacitance, and the film is less resistive than the 100 pF capacitor. A possible reason for this deviation could be the cable used to connect the impedance spectrometer with the sample. Prototype 1, as prototype 2, uses coaxial cables, unlike the reference blue probe that uses standard cables without a shield.

Moreover, a significant noise increase can also be seen for frequency lower than 100 Hz, probably due to the high impedance values, which is difficult for the impedance spectrometer to analyze. However, by cleaning the tips of the GSP and better adjusting its

position, the contact between the probes and the IDE can be improved, reducing this noise at low frequency

4.3.2 DNA

After the validation of our system, a DNA film was deposited on a IDE, as described in section 3.1.1. For the characterization of this DNA thin film, the system was first cooled to a low temperature, and then heated, using the temperature control system previously described, making temperature steps of 20 K starting at 180 K and finishing at 300 K. According to previous data, it was already known that for impedance values below 180 K, only the IDE is being measured, which means that the thin film isn't analyzed under 180 K. So, by starting the measurements at 180 K, it allows us to reduce the total data acquisition time. Before starting this temperature cycle, the film impedance was measured at RT to test if the cooling process induced irreversible changes.

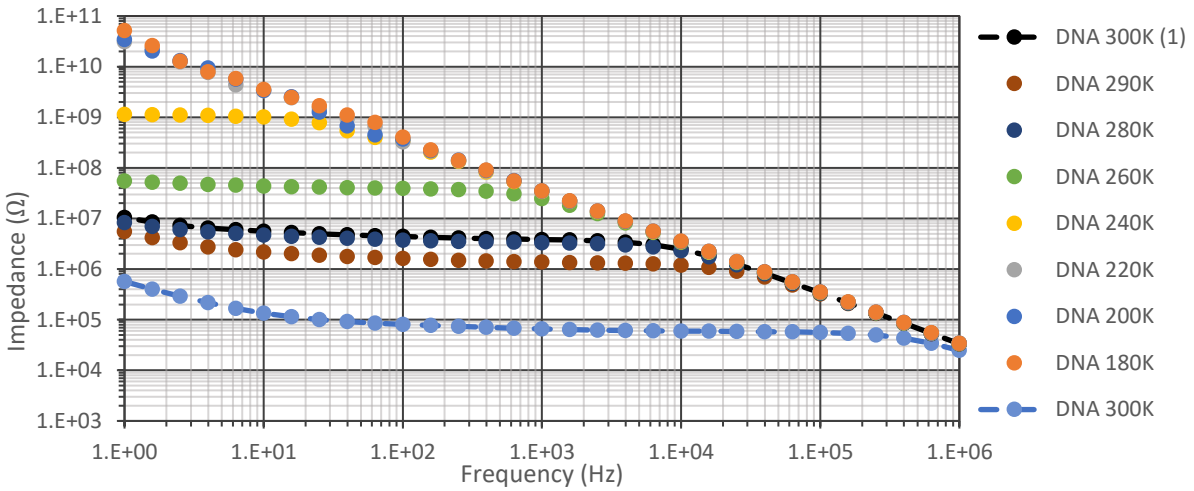

Figure 4.6: Bode plot of impedance at different temperatures for DNA thin film using prototype 1

This data in Figure 4.6 shows that, in the 180-220 K range, the film is much more resistive than the substrate. As a matter of fact, the current applied mainly propagates by the substrate, and the measured values appear to be that of a substrate.

For temperatures above 240 K, the thin film starts to have low enough impedance values to be measured. At high frequencies, the substrate still has a lower impedance than the film, not being possible to measure the thin film properties. For lower frequencies, we can verify that the film presents a resistive (flat part) and a Warburg components (seen by the increase of impedance coming close to 1 Hz, especially for the first measure at 300 K).

Analyzing the data showed that there is a well-defined behavior between the impedance value and the temperature. Although it can be seen in the graph of Figure 4.6 that the

impedance values before (blue dashed lines) and after the cooling process (black dashed lines) at RT, are not the same, the curve after the cooling process being more resistive. To make the data analisis easier, a impedance versus the temperature at a fixed frequency is plotted, as presented in Figure 4.7.

This graph shows that the impedance curve starts from a high value at a low temperature decreasing to a lower one when the temperature increases. However, this behavior changes around 270 K, when the impedance value increases. Because this phenomenon begins at ≈ 270 K ≈ 0°C and after 5h-6h, the curve at 300 K returns to its initial values (not represented in the graph), we conclude that water condensation is the most likely cause for this slope change at ≈ 270 K.

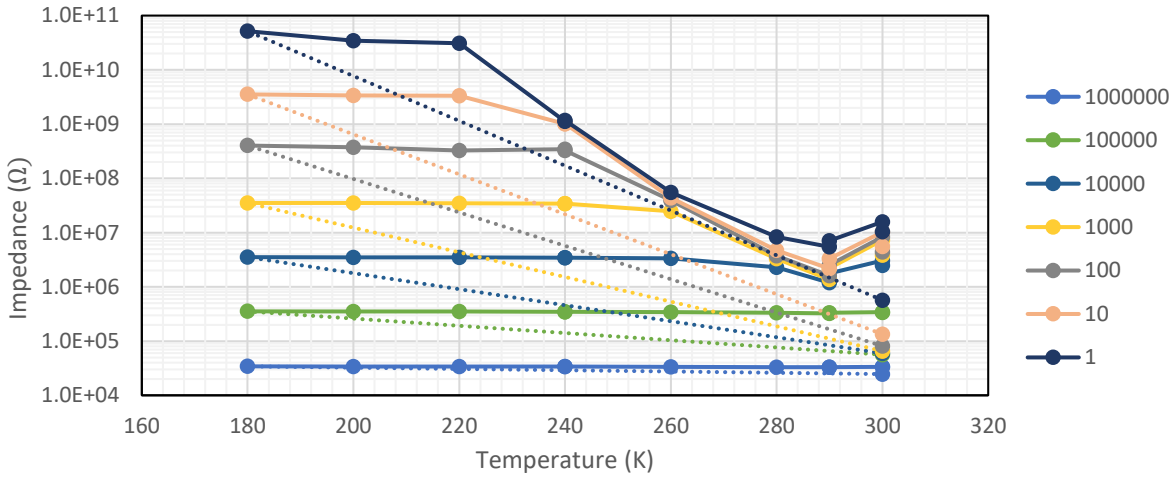

Figure 4.7: Plot of impedance as a function of temperature at different frequencies, for DNA thin film using prototype 1

The most likely cause for this condensation is the acrylic tube, since its two extremities are open, which allows a connection between the inner part of the cryogenic cell and the ambient atmosphere, which is water a source.

To try to limit this phenomenon, foam was placed inside the acrylic tube. Using this method, the foam should limit the water transfer from RT to the cryogenic cell. To observe the impedance variation more precisely, from this point forward, 10 K steps were used in the temperature range. This modification led to the same results as before, so the sample was also protected with teflon tape to avoid condensation on the film itself. Also, to confirm that this phenomenon is due a very slow temperature dynamic in each temperature step two measurements, 5 to 10 min apart, were made in some temperatures to confirm (or not) if the values remain constant for the given temperature. The results obtained in these conditions are displayed in Figure 4.8 and Figure 4.9.

Again, it can see that there is a well-defined behaviour between the impedance components and the temperature. However, there is still a change of slope starting around 270 K and different impedance values at room temperature before and after the cryogenic cooling process.

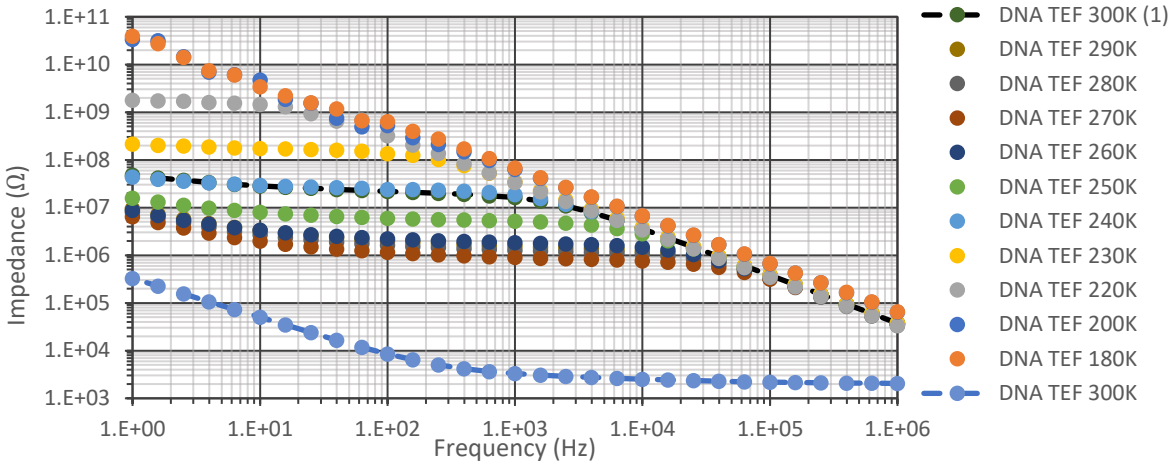

Figure 4.8: Bode plot of impedance at different temperatures, for DNA thin film involved with teflon using prototype 1

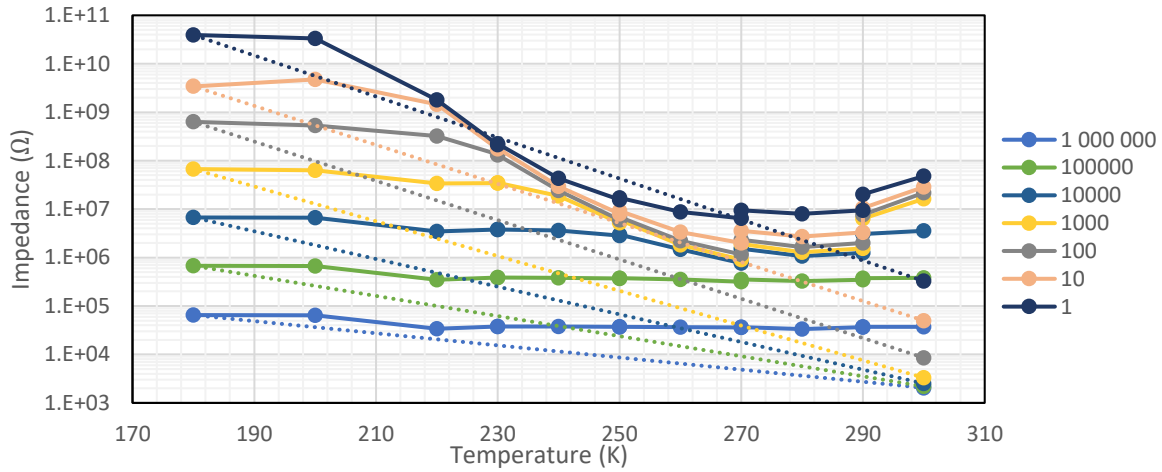

Figure 4.9: Plot of impedance as a function of temperature at different frequencies, for DNA thin film involved with teflon using prototype 1

Without full confirmation, it is still believed that the formation of water is the main reason for the appearance of this phenomenon because the slope starts around 270 K and above, and because the impedance values return to the initial ones after some hours, at room temperature. The graph of Figure 4.10 shows how maintaining the room temperature at the end of the cooling process, the impedance reverts to the initial values. Such results could reinforce the idea that this effect is due to water.

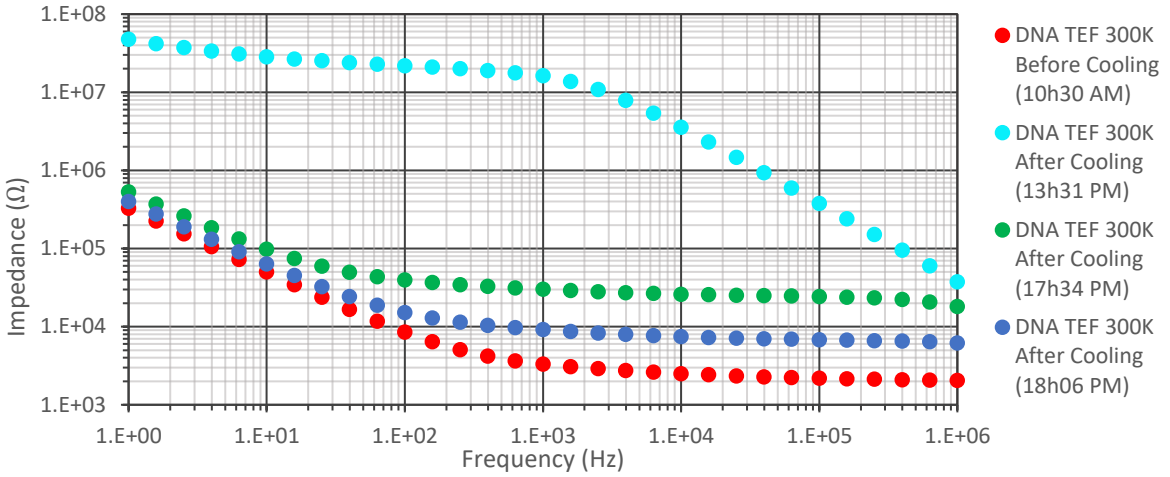

Figure 4.10: Bode plot of impedance as at room temperature, for DNA thin film involved with teflon using prototype 1. Evolution of impedance curves values after cooling process

Analyzing the real and imaginary components of the data is also important, allowing a better understanding of the thin film's properties in the study and finding the film's equivalent circuit model. Using only the bode plot of the DNA, the increasing impedance at low frequency could be attributed to capacitive behavior. Although using the Figure 4.11 Nyquist plot, one can conclude that this is due to the presence of a Warburg effect.

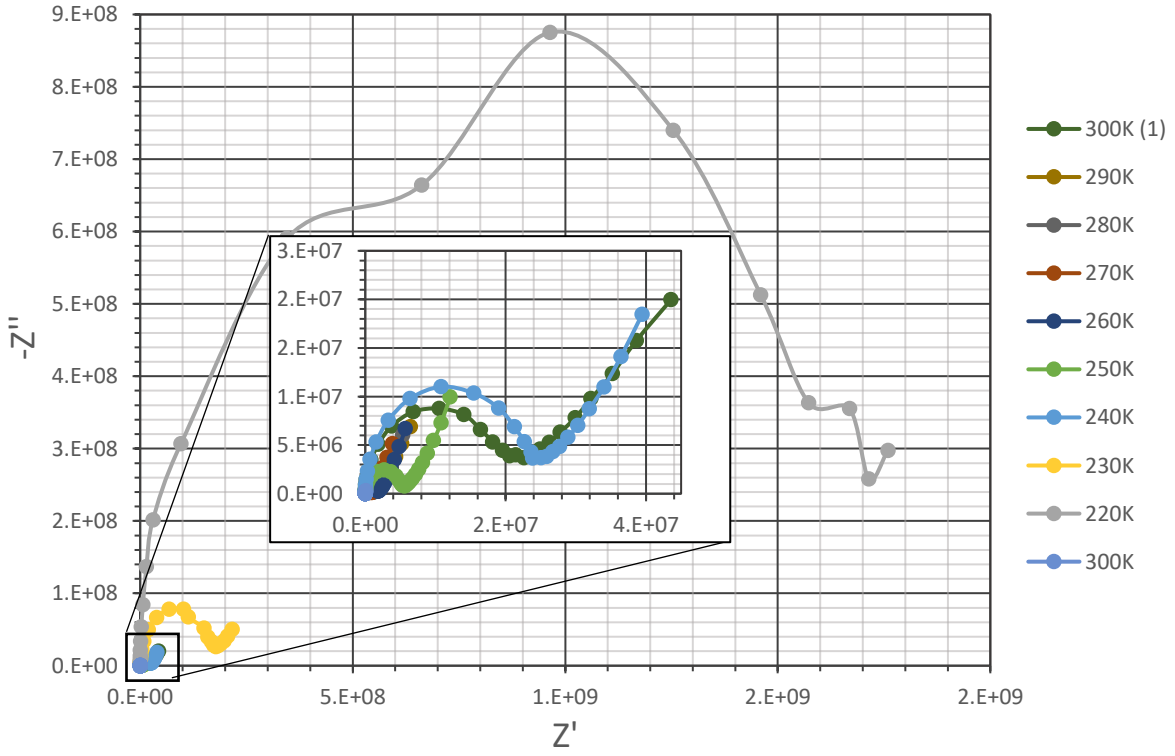

Figure 4.11: Nyquist plot of DNA at different temperatures

In the Nyquist plot of Figure 4.11, for reasons already explained are only represented temperatures above 220 K.

Using the Nyquist and Bode plot data and the software Zview, it is possible to represent electric circuit equivalence to DNA sample, represented in Figure 4.12 and Figure 4.13. This can lead to a better understanding of the DNA components variation with the temperature (Represented the data in Table 4.1). It can also be seen that the Warburg effect occurs at any temperature.

Figure 4.12: Electric circuit equivalence a) The sample b) The DNA film

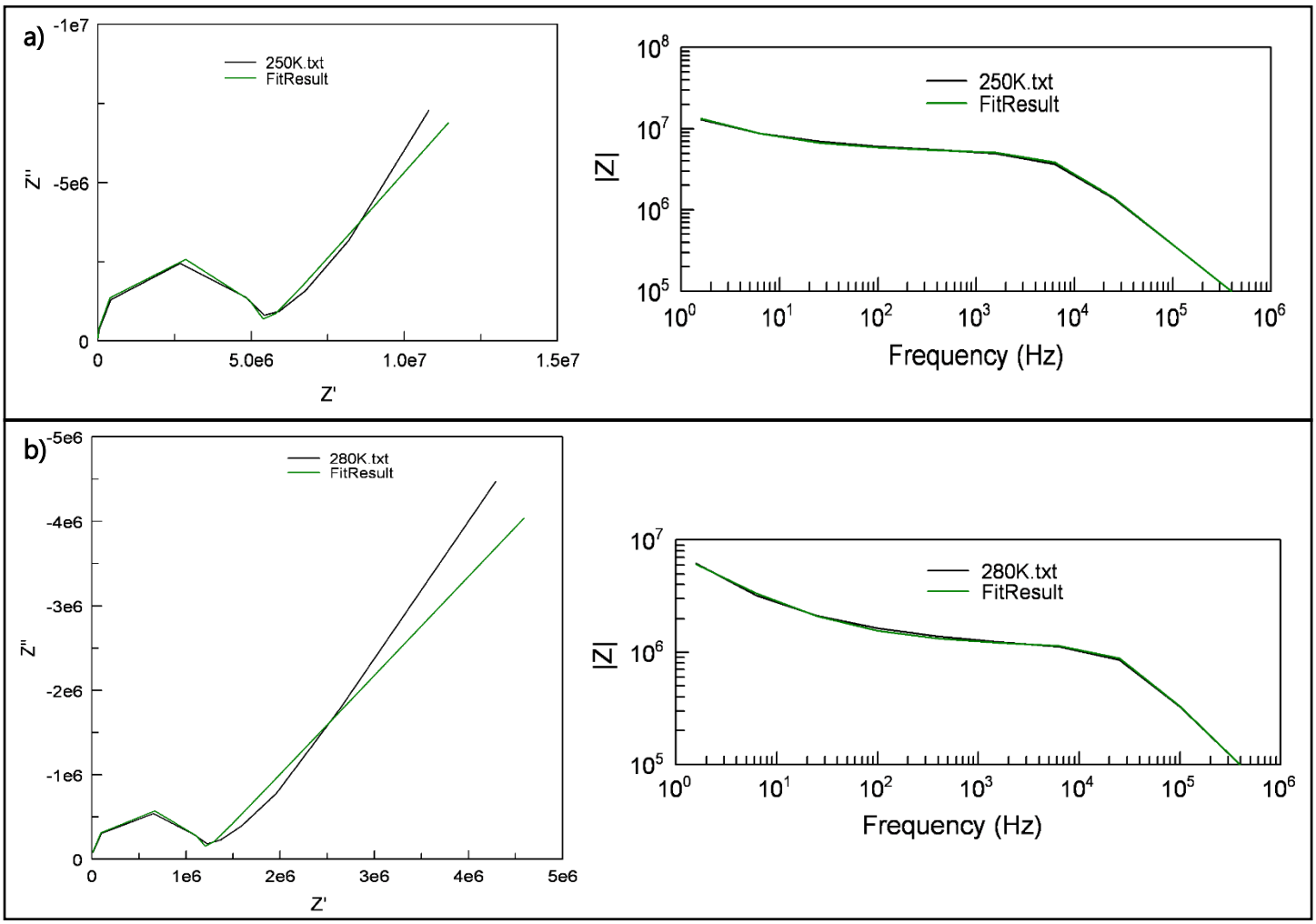

Figure 4.13:ZView graphs of fitting in some temperatures. a) 250K b) 280K

Table 4.1: Equivalent circuit film DNA component values, obtained using Zview software

			Warburg		
Temp (K)	**C_{IDE}**	**R_{Film}**	**W_{Film-R}**	**W_{Film-T}**	**W_{Film-P}**
300 (Before cooling)	-	2.07E+03	4.63E+05	5.8	0.5
220	4.6E-12	1.49E+09	2.25E+09	5.8	0.5
230	4.2E-12	1.52E+08	5.47E+08	5.8	0.5
240	4.2E-12	2.28E+07	1.79E+08	5.8	0.5
250	4.3E-12	5.10E+06	8.28E+07	5.8	0.5
260	4.4E-12	1.67E+06	4.93E+07	5.8	0.5
270	4.3E-12	1.74E+06	5.28E+07	5.8	0.5
280	4.6E-12	1.14E+06	4.58E+07	5.8	0.5
290	4.3E-12	1.37E+06	5.47E+07	5.8	0.5
300 (1)	4.3E-12	1.97E+07	2.24E+08	5.8	0.5

In every temperature, except the first measurement at RT before the cooling process, appears the capacitance component corresponding to the IDE, being the circuit equivalence, the circuit a) of Figure 4.12. In the first RT measurement the circuit equivalence is the circuit b) of Figure 4.12.

The data in Table 4.1 shows that the values of the capacitor are constant, throughout the range of temperatures, just like W_{Film-T} and W_{Film-P}. Something that was expected since the IDE is not supposed to be affected by the temperature, and W_{Film-T} and W_{Film-P} are intrinsic characteristics of the thin film and Warburg effect (section 2.2.1.1).

The R_{Film} values decrease when the temperature increases, meaning that the colder the film is, the more resistive it becomes. However, from the steps of 260 K to 300 K, the behavior doesn't seem so clear. Also, R_{Film} is different before and after the cryogenic process and doesn't present the same values, reinforcing that "something occurs" around 270 K. The W_{Film-R}, has a symmetric value variation with the R_{Film}, as expected and explained in section 2.2.1.1.

4.3.3 Graphene Oxide Film

The graphene oxide (GO) thin film was deposited, as described in section 4.3.3. Before executing the low temperature measurements, the thin film was measured with prototype 1 and the reference blue probe at room temperature, in which both probes data were coincident.

Repeating the same process made with the DNA film, the impedance of the GO film was measured in 180 K - 300 K temperature range. The data are displayed in the Figure 4.14 and Figure 4.15.

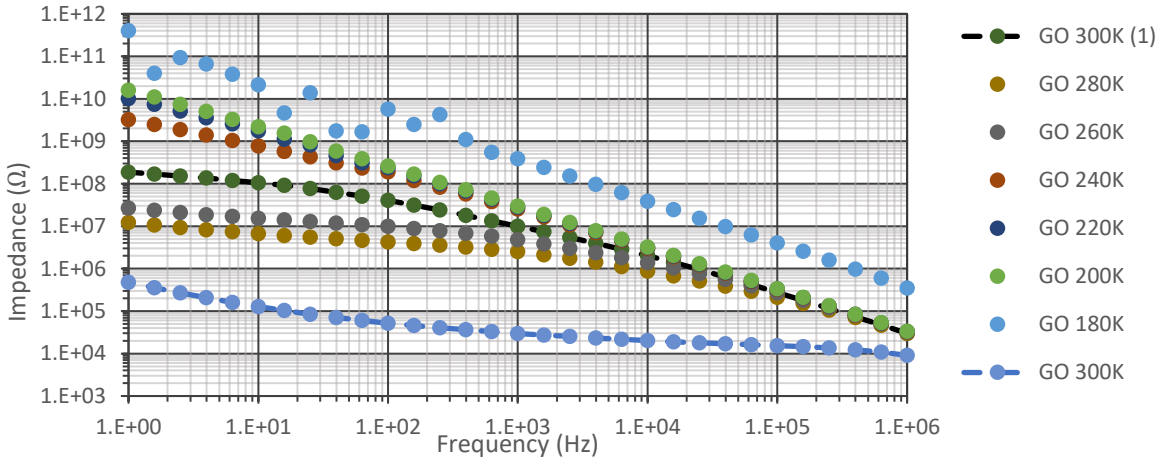

Figure 4.14: Bode plot of impedance at different temperatures, for GO thin film using prototype 1

These results show a similar behavior in the Bode plot to that obtained with the DNA. For temperatures under 220 K, the film is too resistive, only measuring the IDE, and for temperatures above 220 K, reduced slope areas can be seen.

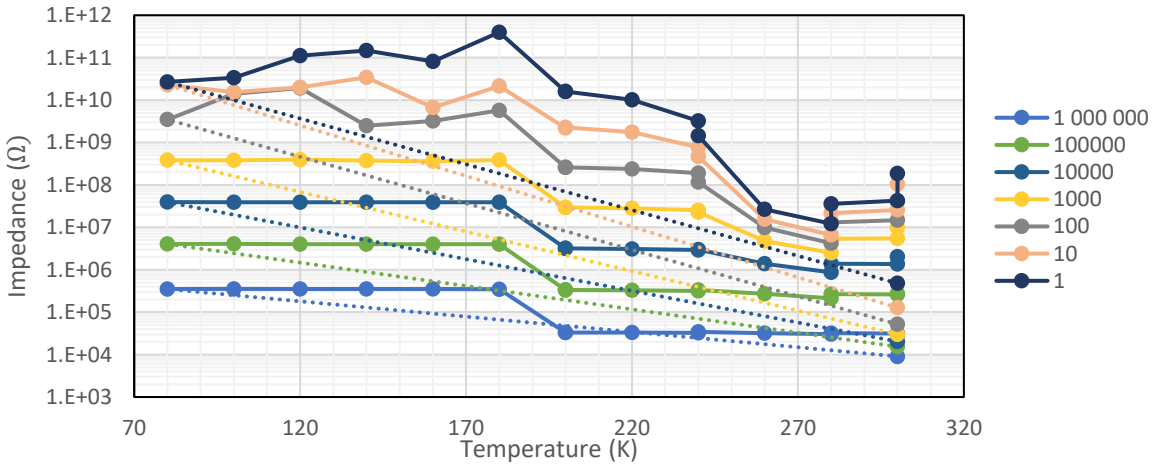

Figure 4.15: Impedance as a function of temperature at different frequencies, for GO thin film using prototype 1

It is important to note that, similarly to the DNA sample, the data obtained for the GO film also ends up with values higher at 300K than before the cooling process. Recovering its original RT values after resting at ambient temperature for five to six hours (not represented in the graph). Also, it's seen in Figure 4.15 that the slope changes around 270 K, becoming positive and even more accentuated than when performing measurements with the DNA.

Since this phenomenon occurs no matter the film, we can conclude that its origin comes from the prototype assembly. Although this phenomenon does not occur when only analyzing the substrate (Figure 4.5).

4.4 Prototype 2 Measurements

The Prototype 1 measurements, as seen above, are not very reliable in the heating process above 270 K and do not have the same impedance values at RT before and after the cooling process, although it returns to its original values after resting for some hours. Due to these facts, it is believed that the origin of these problems is the condensation of water inside the cryogenic cell. So as an attempt to fix these problems, prototype 2 was built as specified in the section 3.4.3. This prototype was also developed, in such a way that it is no longer necessary to monitor the liquid nitrogen level.

4.4.1 Substrate

As for the first assembly, we started by measuring the IDE alone to ensure that its impedance does not variate with the temperature, obtaining the results displayed in Figure 4.16. As in Prototype 1, the data is completely superposed, indicating that the substrate does not present variation with the temperature, as expected. This USB-adapted probe shows less noise at low frequency then Prototype 1, thanks a better contact area.

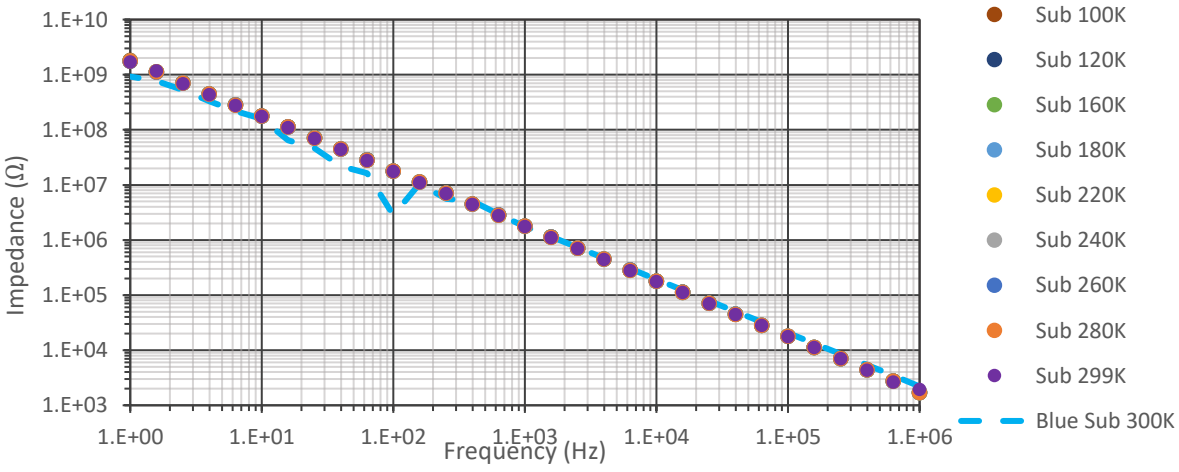

Figure 4.16: Bode plot of substrate at different temperatures, using prototype 2

Unlike Prototype 1, the USB probe used in Prototype 2 didn't suffer a deviation, although such deviation was expected as it did on the graph in Figure 4.3. This assembly lost

the parasite capacitance, returning to the original values for some unknown reason. But as said before, this phenomenon does not affect the measures of the thin film.

4.4.2 DNA (1st Cryogenic Cell Version)

The same film of DNA used in prototype 1 was measured in this new system (section 3.4.3.1). With this system a slightly different approach was used. Instead of only measuring while heating, measurements were also obtained while cooling.

During the measurements, two significant problems were observed in the first controlled temperature level at 280 K (Figure 4.17, t<100 min). First, sensor A and sensor B, placed in the cryogenic cell as represented in Figure 3.21, present a large temperature difference, meaning there is no temperature uniformization along the cell. Second, the curve values obtained at 280 K, no matter which sensor was used as the controller, presented curves that were only expected to appear at 240 K (Figure 4.18), according to the data obtained in prototype 1. These results indicate a lousy temperature gradient in the cell.

The experiment was repeated to confirm if those two problems were not directly correlated. However, in this case, the system was left to warm on its one, instead of using electrical power to control the sample holder temperature. This was obtained by removing the system from the liquid nitrogen and letting the room temperature warm the prototype. The Figure 4.17, shows for t>130 min that with such a process, the temperature in the cell becomes uniform. Unfortunately, with such a process, we cannot make the different temperature steps, but we can confirm if the two problems are correlated. The data measured during a slow temperature drift are displayed in Figure 4.19, Figure 4.20, and Figure 4.21.

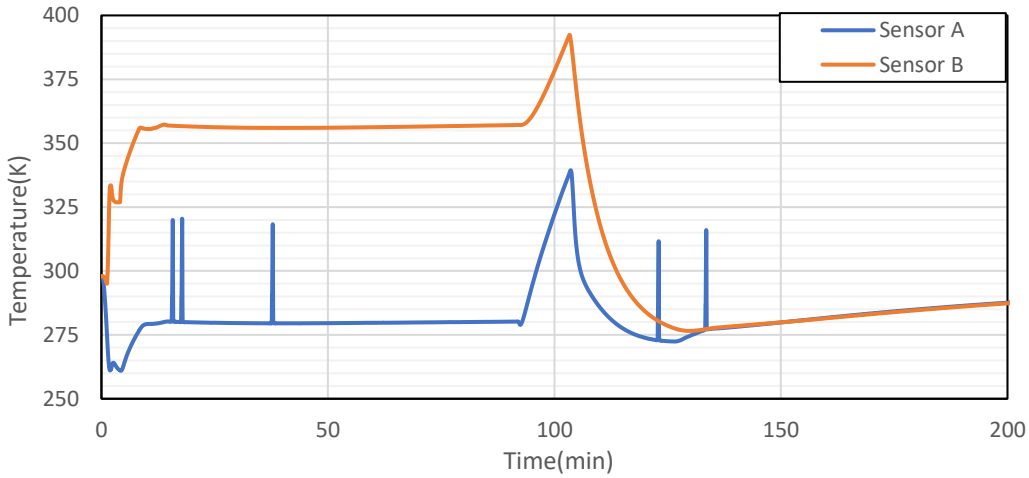

Figure 4.17: Temperature variation of sensors Pt100 A and B during the develop of this experiment with DNA using the prototype 2

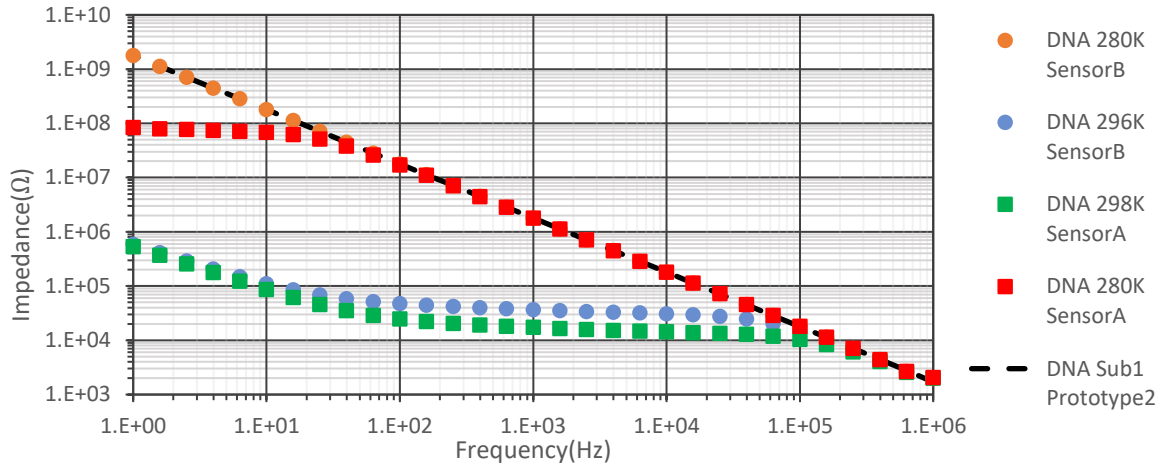

Figure 4.18: Bode plot of DNA thin film at different temperatures, using prototype 2

Comparing these new data with the ones obtained by prototype 1, we can confirm that the data are similar, without the issue appearance present when the temperature is controlled. Meaning the lack of temperature uniformization is the main reason why this sample holder could not acquire the expected data when stabilizing the temperature. Also, the air-tight system fixed the problem detected in prototype 1 (impedance values different, at 300K, before and after the cooling cycle). This result indicates that this issue is related to some condensation. With this in mind, developing a new cryogenic cell is necessary to correct this problem of non-uniform temperature along the sample holder (annex A.2).

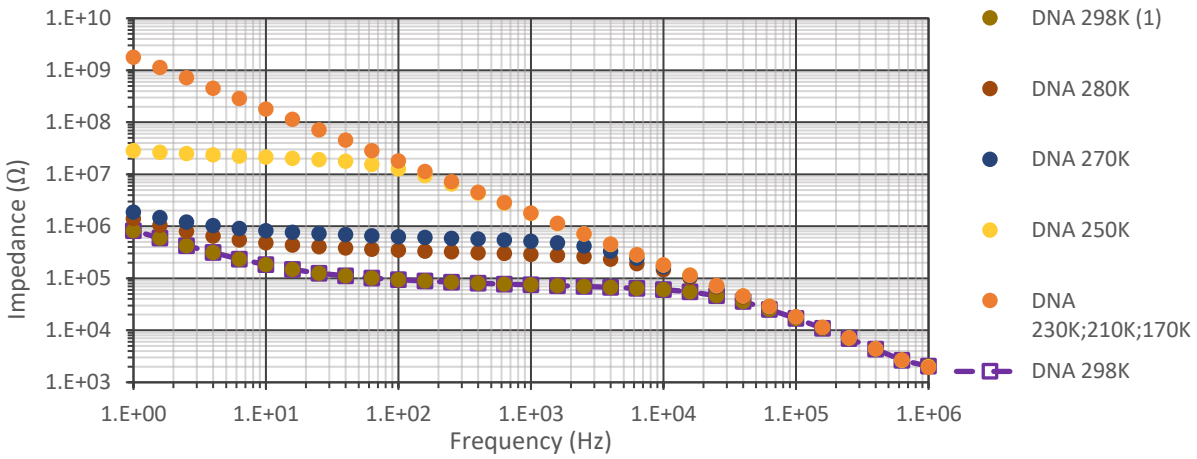

Figure 4.19: Bode plot at different temperatures for DNA film using prototype 2 1st version while heating without temperature control

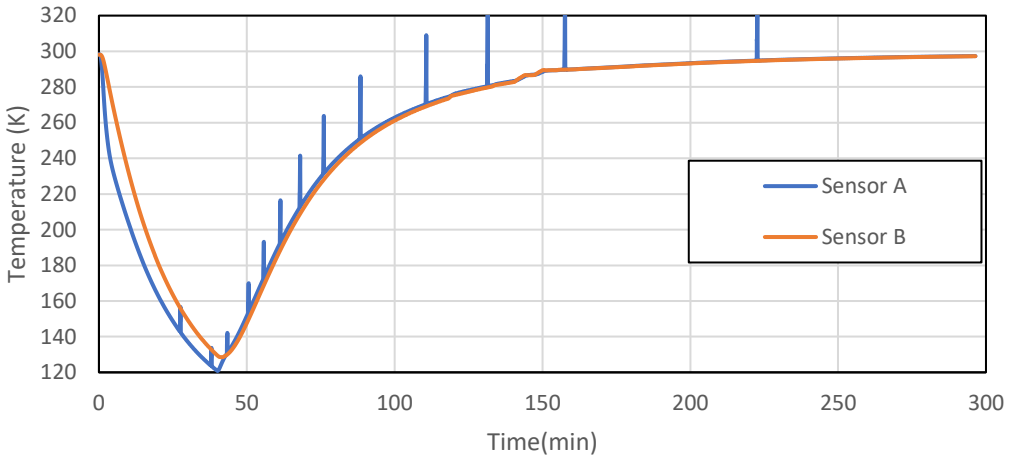

Figure 4.20: Temperature variation of sensor A and B for DNA, using the prototype 2 1st version, without temperature control. The temperature spikes indicate an impedance measurement (data in Figure 4.8)

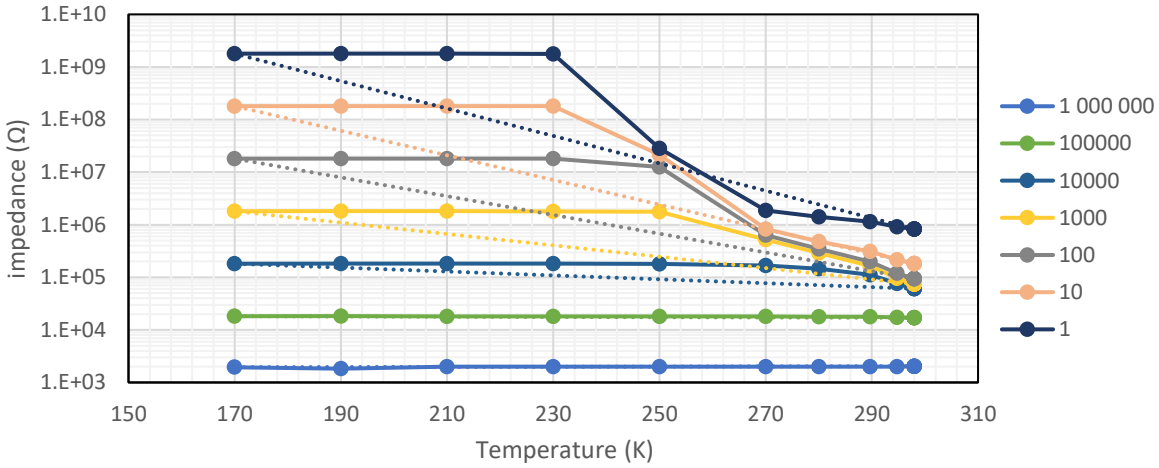

Figure 4.21: Impedance as a function of temperature for DNA film at different frequencies, using prototype 2 1st version without temperature control.

4.4.3 DNA (2nd Cryogenic Cell Version)

To bypass the main drawbacks, present in the previous version, a simpler sample holder version was built, as shown in Figure 3.24, trying to obtain some useful measurements with the sample holder described in section 3.4.3.2. The experiment with the DNA film was repeated, making temperature steps on the cooling and heating, as displayed in Figure 4.22 and Figure 4.23.

During the execution of this experiment, the heating resistor burned before reaching the last two temperature levels, making it impossible to make the last temperature steps (280 K and 300 K). In opposition to the measurement made in the first version of this sample holder, the temperature was measured as uniform in the cryogenic cell (TA=TB). However, the measured curve values are not the expected ones, considering previous data (Figure

4.19), since the capacitive curve starts to appear after 280K instead after 250K as expected. And since the only curves that presented resistive components are the 280K and 300K, we cannot confirm if this behavior continues in the heating process.

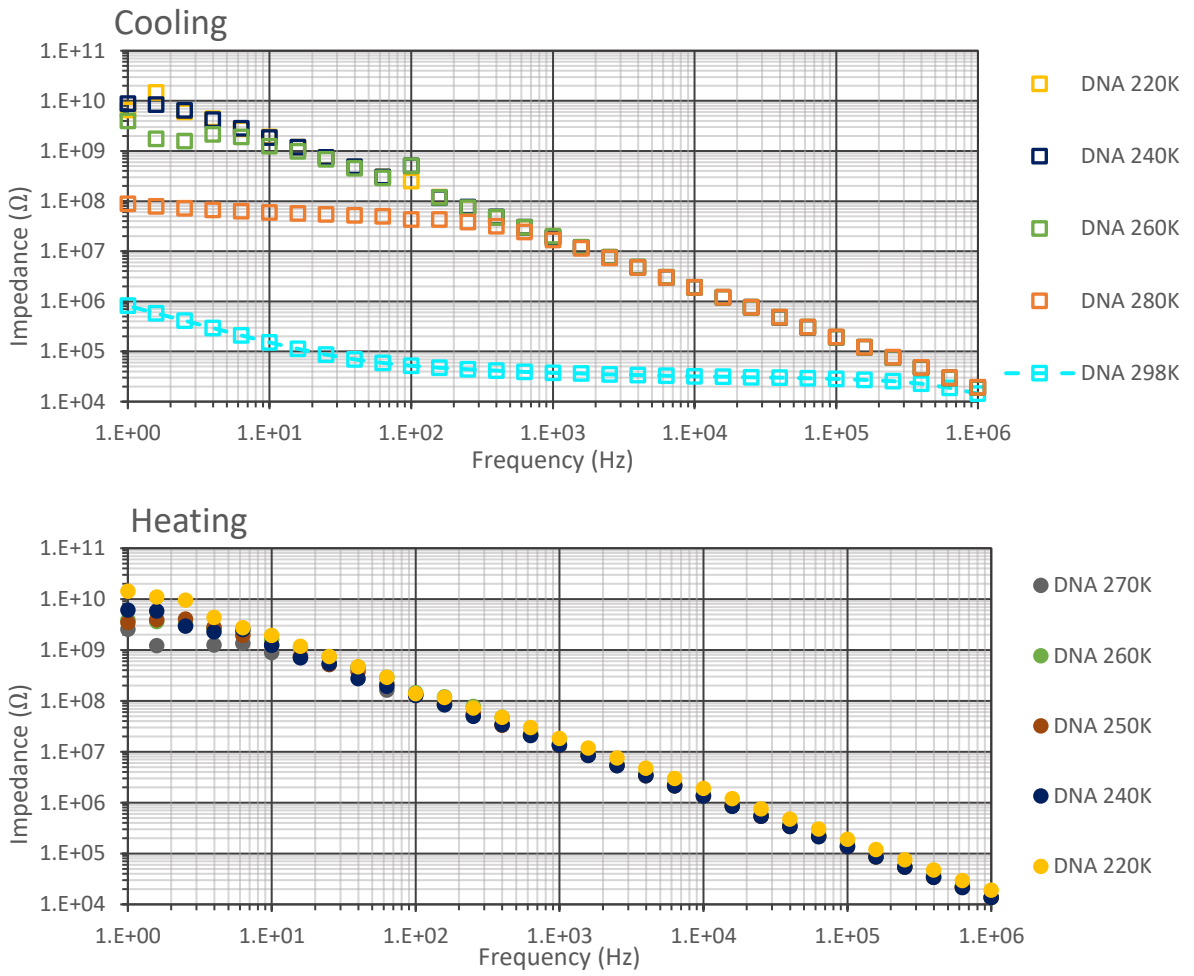

Figure 4.22: Bode plot at different temperatures for DNA film using prototype 2 2nd version. On top the measurements when colling and below the measurements when heating

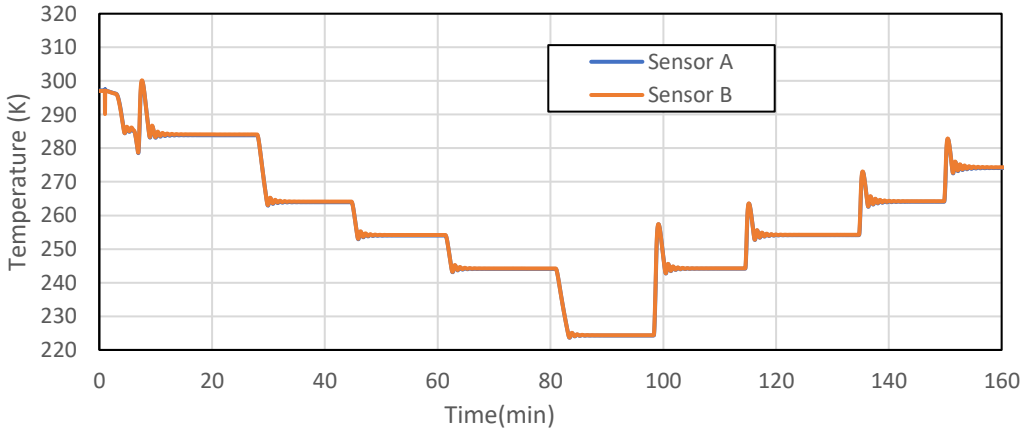

Figure 4.23: Temperature variation of sensor A and B for DNA, using the prototype 2 2nd version.

There are two possible reasons for this set of data. First, since the USB probe is not well fixed, the probe could have shifted, no longer measuring the film. This could only be confirmed if the impedance data for 280 K and 300 K was obtained. Second, this thin film of DNA being the same that was used in all previous measurements, it's possible that the film may be degraded, leading to a different value for the impedance. A final version of this sample holder is designed in A.2.

4.5 Prototype 3 Measurements

Prototype 3 was built to study DC sheet resistance instead of AC impedance. For that, is used the sample holder, seen in Figure 3.25 a) and b), and samples with a completely different structure, no longer using interdigitated samples. In this prototype, two types of substrates were studied: Indium-doped Tin Oxide (ITO) and Fluorine-doped Tin Oxide (FTO).

For these measurements, it was used the power source RIGOL DP811A and a software developed in another thesis [15].

Two methods were used when measuring the sheet resistance of the samples: manual and automatic. In the manual measurements, the data is constantly being measured, while the cryogenic cell is being cooled. In the automatic measurements, a ramp is used of currents with 10 levels from 0 A to 0.071 A, using the V-I slope to obtain the sheet resistance value, when the sample achieves a stable temperature, starting at 300 K and decreasing in jumps of 10 K. Unfortunately, due to limitations during the development of the experiment, due to lack of contact between the sample and the probes, at low temperature, it was not possible to measure under 210 K for the automatic method and under 180 K for the manual method.

4.5.1 ITO Sheet Resistance

Before cooling the system, the sample was measured at room temperature and compared with the tabulated value of 20±6 Ω/□ [16], obtaining value 19.95 Ω/□ for automatic measurement and 19.18 Ω/□ for manual measurement. Since the values obtained are inside the tabled value interval, we can conclude that the system is working properly.

The data obtained for various current intensities are displayed in Figure 4.24. Analyzing the data, we can see no sudden sheet resistance change and that the sheet resistance uniformly decreases when the temperature drops.

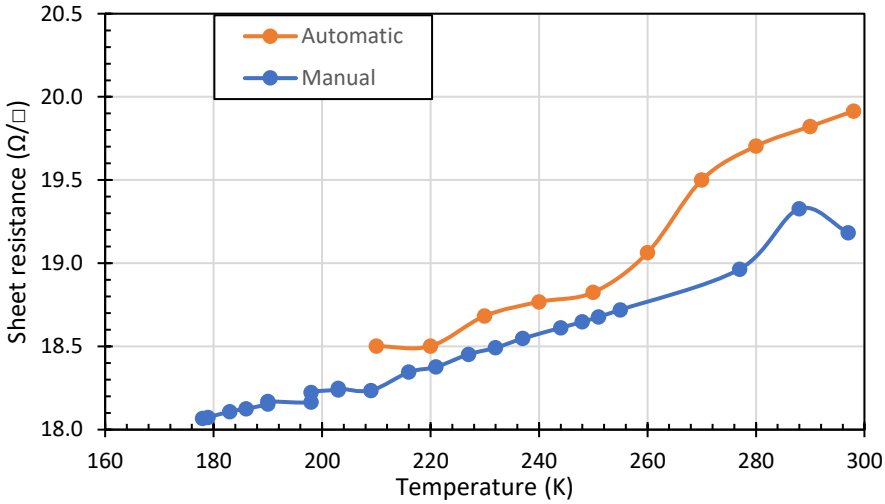

Figure 4.24: ITO sheet resistance as a function of temperature at

4.5.2 FTO Sheet Resistance

The same process used to measure the ITO sheet resistance was applied to the FTO. So, before cooling the system, the sample was measured at room temperature and the sheet resistance value obtained (14.17 Ω/□) was compared with tabulated values (12 to 14 Ω/□) [17]. The values obtained is not inside the tabulated value interval, although very close, this could be because the FTO original sample was cut smaller, to fit in the sample holder. The cutting process is believed to have slightly changed the resistance of the sample.

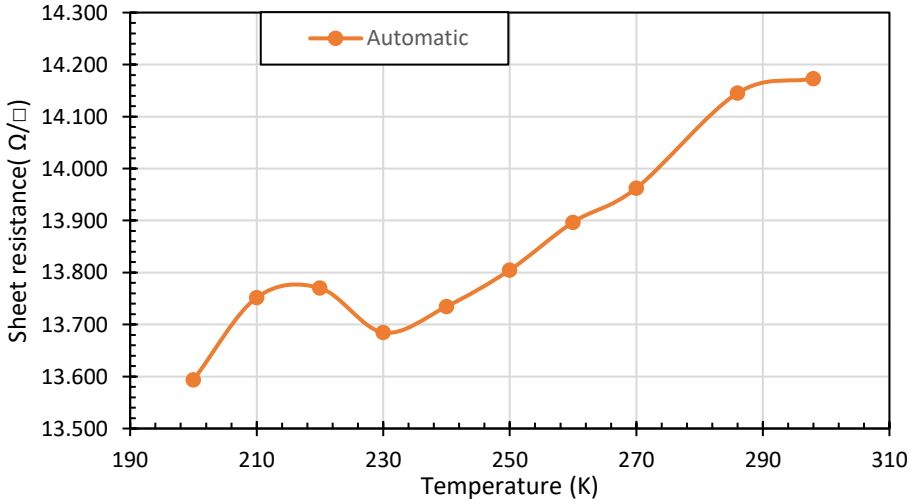

Figure 4.25: FTO sheet resistance as a function of temperature

Analyzing the data in Figure 4.25, we can see that there is no sudden sheet resistance change and that the sheet resistance decreases regularly with the decreasing temperature, except with the measure at 210 K and 220 K.

During the development of the ITO and FTO data acquisition, sometimes the values started to be very resistive due to the displacement of the probe's connector (Figure 3.25) when the system was cooled, moving away the probes from the sample. This problem was fixed by increasing the plastic piece thickness and squeezing this piece more firmly.

To improve this sample holder, a new piece was designed to fix the probes in an easier way to the cryogenic sample holder (Annex B.4). Also, a piece was developed to install the probes in a configuration capable of making volume measurements (Annex B.5). However, with the time remaining it was not possible to build these two new pieces.

5

Conclusions and Future Perspectives

In this work were developed systems capable of making precise temperature control at low temperatures (between 77 K and 300 K) using liquid nitrogen to measure different electrical characteristics in thin films. For that purpose, were developed a thermal barrier allowing a stable temperature control, a LabVIEW program connected to a temperature controller and three different prototypes. Prototypes 1 and 2 were designed to measure the thin film impedance in interdigitated substrates, whereas prototype 3 was dedicated to measure the film sheet resistance.

For prototype 1, we start with a system which was not designed for temperature control. So, we used a temperature controller to monitor and control the sample holder temperature and a "low cost" thermal barrier located around the cryogenic cell to avoid direct contact between the cell and the liquid nitrogen. This assembly can be considered a success because a very good temperature control was obtained, allowing it to make different temperature steps in a quite reasonable amount of time: cooling down to 80 K and heating up to 280 K with 11 temperature stabilized steps in 140 min. Unfortunately, this prototype has two defaults. First, it is necessary to monitor the liquid nitrogen levels (to ensure a rapid cooling process and to avoid direct contact between the liquid nitrogen and the upper part of the cell). Second, the system is not airtight, allowing some water condensation, that could induce some parasitical effects during measurements.

In Prototype 2 the issues presented in prototype 1 have been corrected. In this system, the cryogenic cell is enclosed in an airtight volume, minimizing the water condensation effects. In doing so it was possible to fix the original defaults present in prototype 1. However, this system still presented some problems in temperature homogenization along the cryogenic cell, which makes the system's measurements incorrect. Due to lack of time, it was not

possible to fix this problem but a sample holder that should not present such a problem anymore was designed, making this system fully operational at any temperature (annex A.2).

Prototype 3, instead of measuring the impedance of a thin film, it measures sheet resistance. This system has a structure similar to prototype 1, so it also has the disadvantage of needing monitorization of the liquid nitrogen level. This system can be considered a success because it can make different temperature levels and measure the sheet resistance of different samples.

To improve the data analysis of electric characteristics measured at low temperatures, the communication between the controller 332 and the impedance spectrum analyzer can be improved, existing two methods to accomplish that. The first method is to develop a LabVIEW program that not only interacts with the temperature controller but as well the impedance spectrometer. However, let us note that using this approach makes it impossible to use the preamplifier 1296A, defaulting the study of more resistive samples. The second method is to use the software SMaRT which controls the impedance spectrometer, to control the temperature controller Lakeshore 332 as well, since this software has this possibility.

Improving the communication with these two pieces of equipment, allows an easier way to analyze the data and makes it possible to observe a graph of impedance in order of T while the sample is being measured.

It is also essential to finish prototype 2 by building the final sample holder design (annex A.2) and confirm if it resolves the problems detected.

For prototype 3, two new pieces were also designed to replace the "Multiple tip-block holder" piece (annex B.3). One would keep the probes positioned for sheet resistance measurements, but it is steadier than the method used in this thesis (annex B.4). The second piece would allow the prototype to be used for volume resistivity measurements of films (annex B.5).

BIBLIOGRAPHY

[1] A. I. G. Francisco, "Montagem Didática para Medições de Resistividade de Metais na Gama," Setembro 2018.

[2] A. O. d. S. Martins, "Electrical Impedance Measurements of DNA Molecules and Gold Nanoparticles at low Temperatures," Novembro 2019.

[3] instruments, AMETEK scientific, "129610A Cryostat System," Solartron analytical, [Online]. Available: https://www.ameteksi.com/products/materials-analysis-accessories/129610a-cryostat-system. [Accessed 13 08 2022].

[4] analytical, Solartron, *129610A LHe/LN2 Cryostat System,* AMETEK, inc, 2016.

[5] X.-Z. Yuan, C. Song, H. Wang and J. Zhang, Electrochemical Impedance Spectroscopy in PEM Fuel Cells, Vancouver, BC, Canada: Springer, 2009.

[6] J. P. Heath, *Simulation of Impedance Spectroscopy in Electroceramics,* The University of sheffield, July 2017.

[7] S.R.Taylor and E.Gileadi, "Physical Interpretation of the Warburg Impedance," *Corrosion,* 1995.

[8] R. Kinder, M. Mikolásek and D. Donoval, "MEASUREMENT SYSTEM WITH HALL AND A FOUR POINT," *Journal of ELECTRICAL ENGINEERING,* vol. 64, no. 2, p. 06–111, 2013.

[9] "Resistência de folha," WikiLand, [Online]. Available: https://www.wikiwand.com/pt/Resist%C3%AAncia_de_folha. [Accessed 09 08 2022].

[10] Metrohm, *InterDigitated Gold Electrodes,* DropSens.

[11] Instruments, AMETEK Scientific, "1260A Frequency Response Analyzer," Solartron, [Online]. Available: https://www.ameteksi.com/products/frequency-response-analyzers/1260a-impedance-gain-phase-analyzer. [Accessed 14 08 2022].

[12] Instruments, AMETEK Scientific, "1296A Dielectric Interface System," Solartron, [Online]. Available: https://www.ameteksi.com/products/materials-analysis-accessories/1296a-dielectric-interface. [Accessed 14 08 2022].

[13] Lake Shore Cryotronics, User's Manual Model 332 Temperature Controller, USA: Lake Shore Cryotronics, Inc., 2009.

[14] OHMITE, TCH Series, "35 Watt TO220 Package Thick Film Power," [Online]. Available: https://www.ohmite.com/assets/docs/res_tch35.pdf.

[15] L. Gaboleiro, "Desenvolvimento de sistema de caracterização elétrica de dispositivos finos," September 2022.

[16] P. G. &. O. GmbH, "ITO Coatings," Präzisions Glas & Optik GmbH, [Online]. Available: https://www.pgo-online.com/intl/ito.html. [Accessed 27 08 2022].

[17] D. Carreira, P. Ribeiro, M. Raposo and S. Sério, "Engineering of TiO2 or ZnO—Graphene Oxide Nanoheterojunctions for Hybrid Solar Cells Devices," Photonics, 2021, 8, 75.

A

Appendix A: prototype 2

A.1 Cryogenic sample holder prototype 2

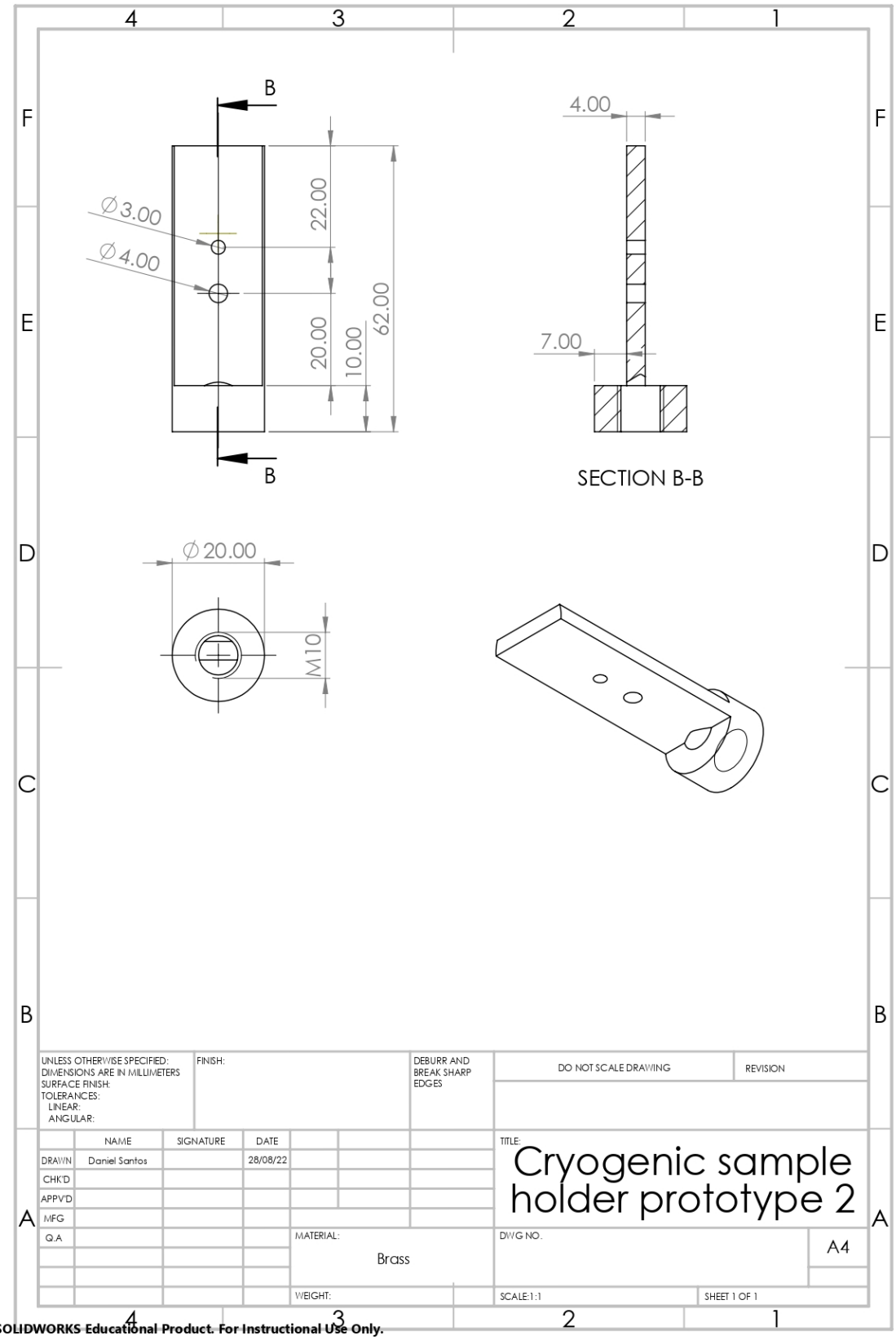

A.2 Final sample holder prototype 2

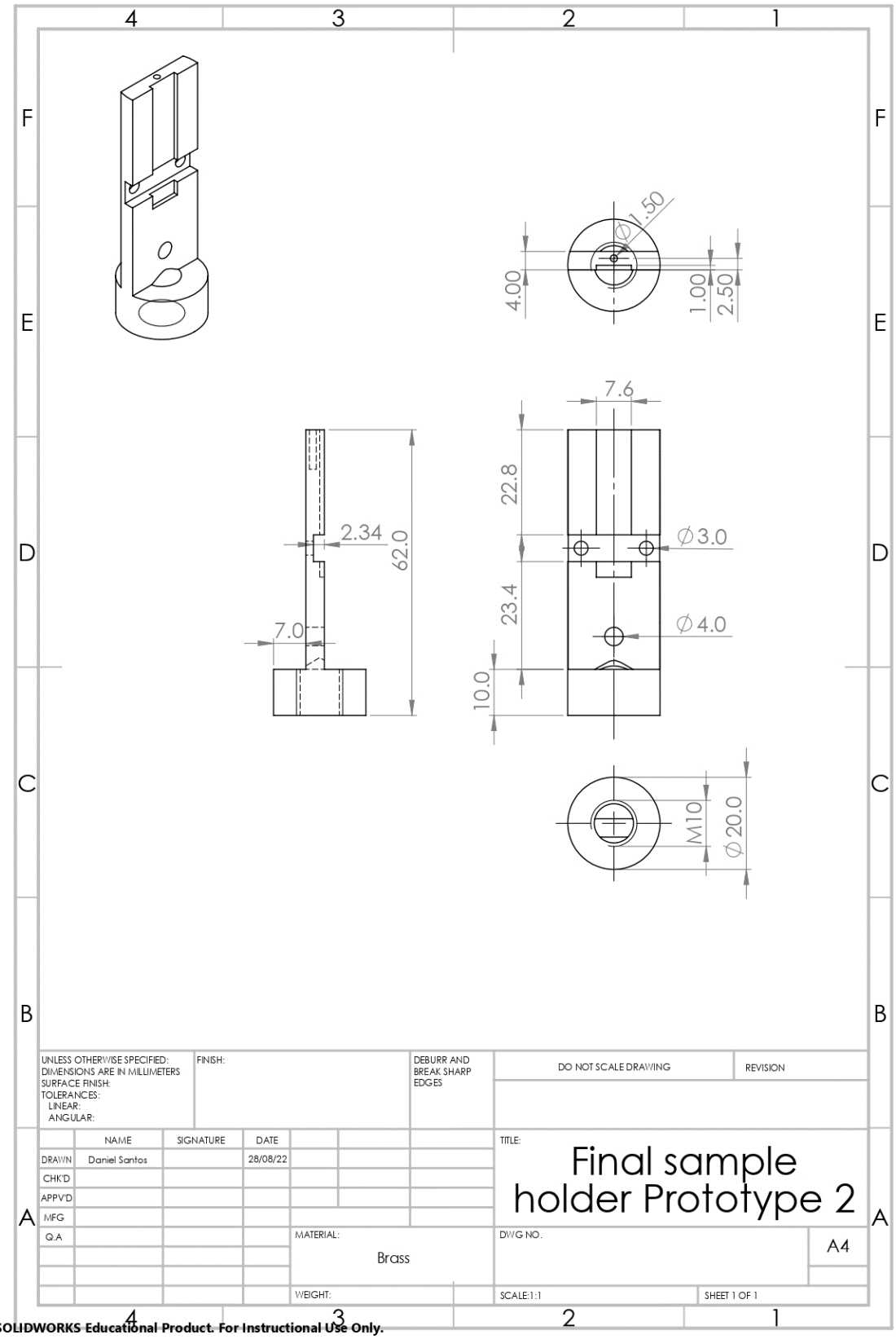

B

APPENDIX B: PROTOTYPE 3

B.1 Base sheet resistance

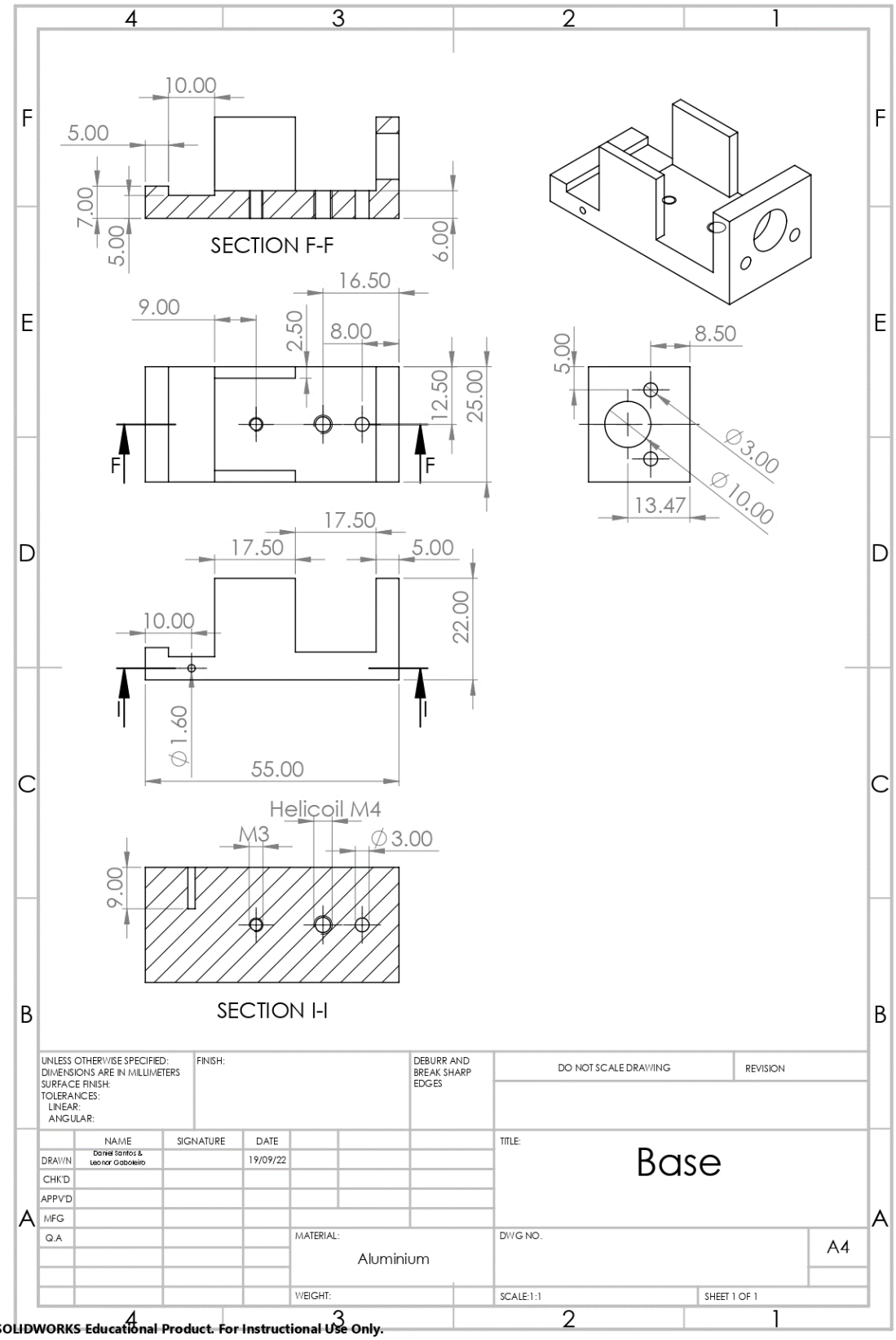

B.2 Connector holder sheet resistance

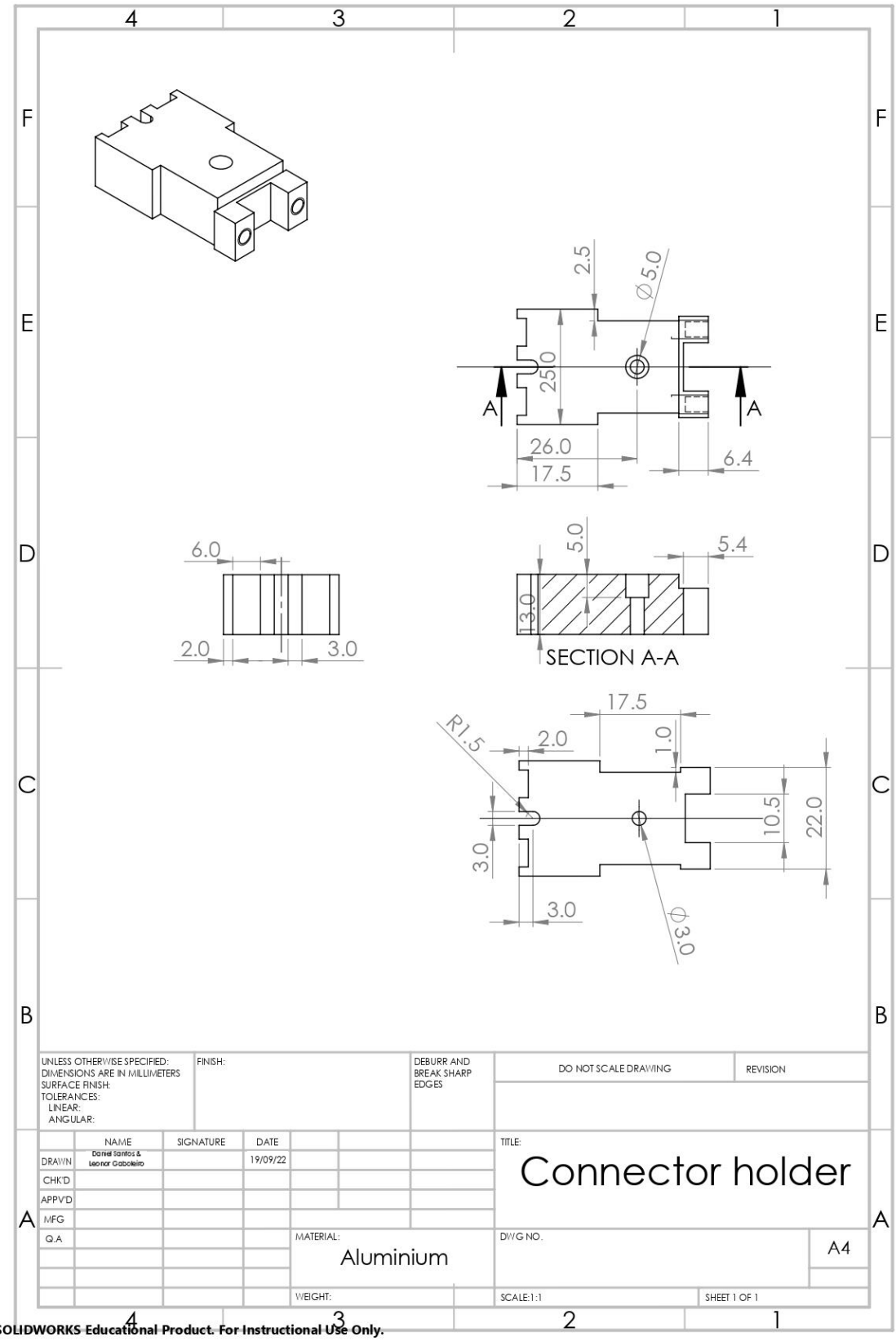

B.3 Connector clamping

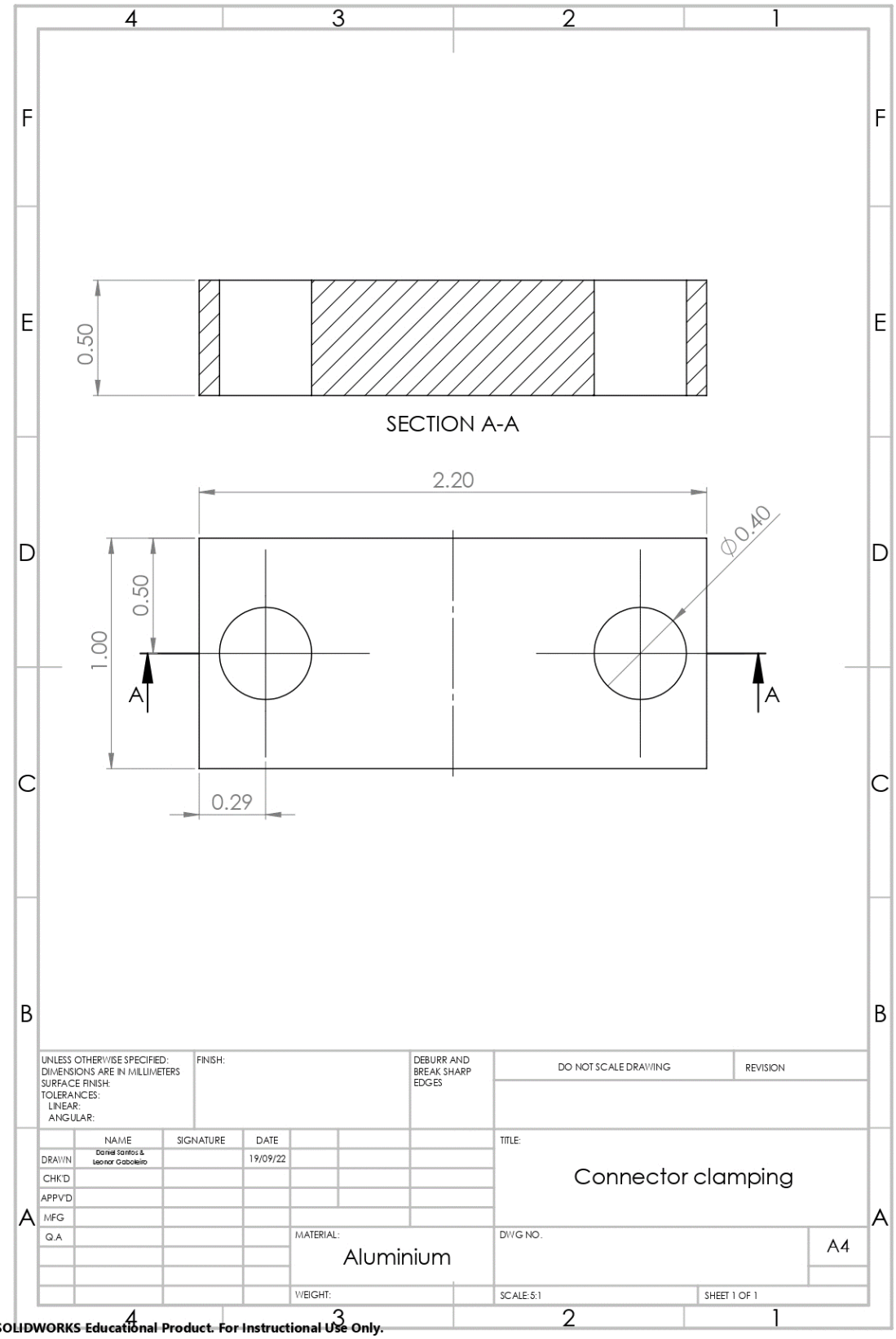

B.4 Cryogenic tip holder for surface measurements

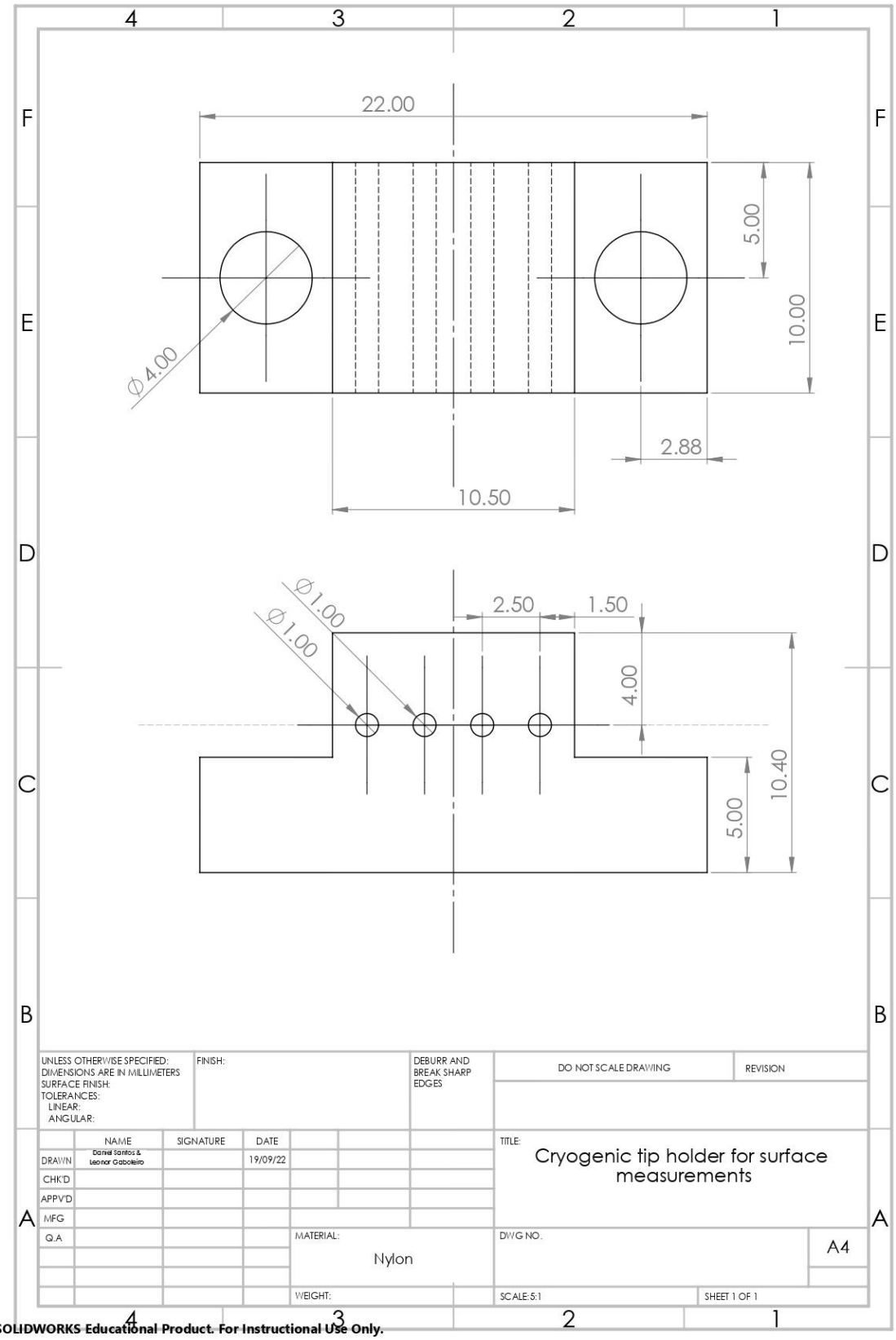

B.5 Cryogenic tip holder for volume measurements